

Journal of Visualized Experiments

Uniaxial Compression Experiment of CO₂-bearing Coal Using the Visualized and Constant Volume Gas-solid Coupling Test System --Manuscript Draft--

Article Type:	Methods Article - JoVE Produced Video
Manuscript Number:	JoVE59405R1
Full Title:	Uniaxial Compression Experiment of CO ₂ -bearing Coal Using the Visualized and Constant Volume Gas-solid Coupling Test System
Keywords:	carbon dioxide sequestration; gas adsorption; coal sample; sorption-induced damage; fractal characteristic
Corresponding Author:	Hanpeng Wang Shandong University Jinan, Shandong CHINA
Corresponding Author's Institution:	Shandong University
Corresponding Author E-Mail:	sduwhp@126.com
Order of Authors:	Weitao Hou Hanpeng Wang Wei Wang Zhongzhong Liu Qingchuan LI
Additional Information:	
Question	Response
Please indicate whether this article will be Standard Access or Open Access.	Standard Access (US\$2,400)
Please indicate the city, state/province, and country where this article will be filmed . Please do not use abbreviations.	Huainan, Anhui Province, China

TITLE:

A Uniaxial Compression Experiment with CO₂-Bearing Coal Using a Visualized and Constant-Volume Gas-Solid Coupling Test System

AUTHORS AND AFFILIATIONS:

Weitao Hou¹, Hanpeng Wang¹, Wei Wang¹, Zhongzhong Liu¹, Qingchuan Li¹

¹Research Center of Geotechnical and Structural Engineering, Shandong University, Jinan, China

Corresponding author:

Hanpeng Wang (pcwli@163.com)

Email addresses of co-authors:

Weitao Hou (weitaohou@163.com)

Wei Wang (1024435565@qq.com)

Zhongzhong Liu (1019895262@qq.com)

Qingchuan Li (lqcz1989@126.com)

KEYWORDS:

Environmental science, carbon dioxide sorption, coal briquette, real-time image monitoring, uniaxial compression, fractal dimension

SUMMARY:

This protocol demonstrates how to prepare a briquette sample and conduct a uniaxial compression experiment with a briquette in different CO₂ pressures using a visualized and constant-volume gas-solid coupling test system. It also aims to investigate changes in terms of coal's physical and mechanical properties induced by CO₂ adsorption.

ABSTRACT:

Injecting carbon dioxide (CO₂) into a deep coal seam is of great significance for reducing the concentration of greenhouse gases in the atmosphere and increasing the recovery of coalbed methane. A visualized and constant-volume gas-solid coupling system is introduced here to investigate the influence of CO₂ sorption on the physical and mechanical properties of coal. Being able to keep a constant volume and monitor the sample using a camera, this system offers the potential to improve instrument accuracy and analyze fracture evolution with a fractal geometry method. This paper provides all steps to perform a uniaxial compression experiment with a briquette sample in different CO₂ pressures with the gas-solid coupling test system. A briquette, cold-pressed by raw coal and sodium humate cement, is loaded in high-pressure CO₂, and its surface is monitored in real-time using a camera. However, the similarity between the briquette and the raw coal still needs improvement, and a flammable gas such as methane (CH₄) cannot be injected for the test. The results show that CO₂ sorption leads to peak strength and elastic modulus reduction of the briquette, and the fracture evolution of the briquette in a failure state indicates fractal characteristics. The strength, elastic modulus, and fractal dimension are all correlated with CO₂ pressure but not with a linear correlation. The visualized and constant-

volume gas-solid coupling test system can serve as a platform for experimental research about rock mechanics considering the multifield coupling effect.

INTRODUCTION:

The increasing concentration of CO₂ in the atmosphere is a direct factor causing the global warming effect. Due to the strong sorption capacity of coal, CO₂ sequestration in a coal seam is regarded as a practical and environment-friendly means to reduce the global emission of greenhouse gas^{1,2,3}. At the same time, the injected CO₂ can replace CH₄ and result in gas production promotion in coalbed methane recovery (ECBM)^{4,5,6}. The ecological and economic prospects of CO₂ sequestration have recently attracted worldwide attention among researchers, as well as among different international environmental protection groups and governmental agencies.

Coal is a heterogeneous, structurally anisotropic rock composed of a pore, fracture, and coal matrix. The pore matrix has a large specific surface area, which can adsorb a large amount of gas, playing a vital role in gas sequestration, and the fracture is the main path for free gas flow^{7,8}. This unique physical structure leads to a great gas adsorption capacity for CH₄ and CO₂. Mine gas is deposited in coalbed in a few forms: (1) adsorbed on the surface of micropores and larger pores; (2) absorbed in the coal molecular structure; (3) as free gas in fractures and larger pores; and (4) dissolved in deposit water. The sorption behavior of coal to CH₄ and CO₂ causes matrix swelling, and further studies demonstrate that it is a heterogeneous process and is related to the coal lithotypes^{9,10,11}. In addition, gas sorption can result in damage in the constitutive relation of coal^{12,13,14}.

The raw coal sample is generally used in coal and CO₂ coupling experiments. Specifically, a large piece of raw coal from the working face in a coal mine is cut to prepare a sample. However, the physical and mechanical properties of raw coal inevitably have a high dispersion degree due to the random spatial distribution of natural pores and fractures in a coal seam. Moreover, the gas-bearing coal is soft and difficult to be reshaped. According to the principles of the orthogonal experimental method, the briquette, which is reconstituted with raw coal powder and cement, is regarded as an ideal material used in the coal sorption test^{15,16}. Being cold-pressed with metal dies, its strength can be preset and remains stable by adjusting the quantity of cement, which benefits the comparative analysis of the single-variable effect. Additionally, although the porosity of the briquette sample is ~4–10 times that of the raw coal sample, similar adsorption and desorption characteristics and stress-strain curve have been found in the experimental research^{17–20}. In this paper, a scheme of a similar material for gas-bearing coal has been adopted to prepare the briquette²¹. The raw coal was taken from the 4671B6 working face in the Xinzhuangzi Coal Mine, Huainan, Anhui Province, China. The coal seam is approximately 450 m below ground level and 360 m below sea level, and it dips at about 15° and is approximately 1.6 m in thickness. The height and diameter of the briquette sample are 100 mm and 50 mm, respectively, which is the recommended size suggested by the International Society for Rock Mechanics (ISRM)²².

The previous uniaxial or triaxial loading test instruments for gas-bearing coal experiments under

laboratory conditions have some shortages and limitations, presented as follows^{23–28}: (1) during the loading process, the vessel volume decreases with the piston moving, causing fluctuations in gas pressure and disturbances in gas sorption; (2) the real-time image monitoring of samples, as well as circumferential deformation measurements in a high gas pressure environment, is difficult to conduct; (3) they are limited to stimulation of dynamic load disturbances on preloaded samples to analyze their mechanical response characteristics. In order to improve the instrument precision and data acquisition in the gas-solid coupling condition, a visualized and constant-volume test system²⁹ has been developed (**Figure 1**), including (1) a visualized loading vessel with a constant volume chamber, which is the core component; (2) a gas filling module with a vacuum channel, two filling channels, and a releasing channel; (3) an axial loading module consisting of an electro-hydraulic servo universal testing machine and control computer; (4) a data acquisition module comprised of a circumferential displacement measurement apparatus, a gas pressure sensor, and a camera at the window of the visualized loading vessel.

The core visualized vessel (**Figure 2**) is specifically designed so that two adjusting cylinders are fixed on the upper plate and their pistons move simultaneously with the loading one through a beam, and the sectional area of the loading piston is equal to the sum of that of the adjusting cylinders. Flowing through an inner hole and soft pipes, the high-pressure gas in the vessel and the two cylinders is connected. Therefore, when the vessel-loading piston moves downward and compresses the gas, this structure can offset the change in volume and eliminate pressure interference. In addition, the enormous gas-induced counterforce exerting on the piston is prevented during the test, significantly improving the safety of the instrument. The windows, which are equipped with tempered borosilicate glass and situated on three sides of the vessel, provide a direct way to take a photograph of the sample. This glass has been successfully tested and proved to resist up to 10 MPa gas with a low expansion rate, high strength, light transmittance, and chemical stability²⁹.

This paper describes the procedure to perform a uniaxial compression experiment of CO₂-bearing coal with the new visualized and constant-volume gas-solid coupling test system, which includes the description of all pieces that prepare a briquette sample using raw coal powder and sodium humate, as well as the successive steps to inject high-pressure CO₂ and conduct uniaxial compression. The whole sample deformation process is monitored using a camera. This experimental approach offers an alternative way to quantitatively analyze the adsorption-induced damage and fracture evolution characteristic of gas-bearing coal.

PROTOCOL:

1. Sample preparation

1.1. Collect raw coal blocks from the 4671B6 working face from the Xinzhuangzi coal mine. Note that, due to the low strength and looseness of the structure, the raw coal is broken and probably mixed with impurities. To avoid the influence of these internal and external factors, as well as reduce the inhomogeneity of coal as much as possible, select large coal blocks (about 15 cm long, 10 cm wide, and 10 cm high).

1.2. Use a tweezer to remove impurities mixed in the coal and scrub the crusher chamber with absorbent cotton and acetaldehyde.

1.3. Smash the coal blocks into small pieces with a jaw crusher, and shelter them in a sieve shaker equipped with standard screens of 6 and 16 mesh. Place the sorted coal powder separately according to diameter.

1.4. Weigh 1,000 g and 300 g of pulverized coal with a particle size distribution of ~0–1 mm and ~1–3 mm, respectively. Put them together in a beaker in a mass proportion of 0.76:0.24 and mix them well with a glass rod (with a diameter of 6 mm).

NOTE: According to the Gaudian-Schuman function of continuous packing theory, when the particle size distribution value (m) equals approximately 0.25 (mass of particle size is 1–3 mm: total mass = 0.24), the strength of the briquette is maximal³⁰.

1.5. To prepare the cement, put 4 g of sodium humate powder (99.99% purity) into a beaker and add approximately 96 mL of distilled water. Use a glass rod to stir them and make sure that all sodium humate is well dissolved.

NOTE: The concentration of cement directly affects the compressive strength of briquette. **Table 1** reveals specific ratios of briquette preparation, of which the No. 2 sample has been used for the representative results.

1.6. Put 230 g of mixed coal powder and 20 g of sodium humate solution into a beaker and mix them together.

NOTE: Based on previous experiences making samples, a briquette produced with 250 g of material, using the cold press method, meets the size requirement of a standard rock sample²², where coal powder accounts for 92% and cement accounts for 8%.

1.7. Cold-press the briquette using the shaping tools adapted to the size of the briquette (**Figure 3**).

1.7.1. To produce a standard-sized briquette, coat the inner surface of the shaping tools with lubricating oil. Assemble tool components #2, #3, and #4 of **Figure 3**, and fill the hole with 250 g of mixed material.

1.7.2. Put component #1 of **Figure 3** on top of the material, and place everything under the piston of an electro-hydraulic servo universal testing machine.

1.7.3. Launch the software **WinWdw** (or equivalent) to control the electro-hydraulic servo universal testing machine. In the software, click on **Force Range** to set the maximum force to 50 kN, and click on **Reset** to clear the displacement value.

177
178 1.7.4. Left-click on the option **Displacement Loading Rate**. Set the moving ratio at 0.5 mm/min;
179 then, click on **Start**. When the value of the test force is 29.4 kN, set the moving ratio at its lowest
180 value (0.005 mm/min) and press for 15 min. Then, click on **Unload**.

181
182 1.7.5. Take out the shaping tools and invert them onto a rubber plate. Use a rubber hammer to
183 disassemble tool components #4, #2, #3, and #1 in that order.

184
185 1.8. Put the briquette in a 40 °C incubator for 48 h. Then, weigh its mass with electronic scales
186 (with a precision of 0.01 g) and measure its height and diameter with a Vernier caliper (with a
187 precision of 0.02 mm) after drying.

188
189 1.9. Measure the moisture content, ash content, and volatile content of the briquette, using a
190 proximate analyzer (see the **Table of Materials**) at a temperature of 20 °C and a relative humidity
191 of 65% (per standard GB/T 212-2008). Perform a vitrinite reflectance measurement on the
192 polished briquette, using a photometer microscope (per standard GB/T 6948-2008).

193
194 1.10. Measure the uniaxial compressive strength, tensile strength, cohesion, and internal friction
195 angle, using a universal testing machine and a strain controlled direct shear apparatus (per
196 standard GB/T 23561-2010). Perform a Poisson ratio measurement using a resistance strain
197 gauge (per standard GB/T 22315-2008).

198
199 1.11. Conduct an adsorption test of the raw coal and the briquette, using an isotherm adsorption
200 instrument (per standard GB/T19560-2008).

201 202 **2. Experimental methods**

203 204 **2.1. Laboratory setup**

205
206 2.1.1. Place the test system in a quiet, vibration-free area of a clean laboratory without
207 electromagnetic interference. The room temperature should remain stable during the test.

208
209 2.1.2. Put the visualized vessel on the platform of the electro-hydraulic servo universal testing
210 machine. Connect the piston of the testing machine with that of the visualized vessel with the
211 use of a specific tool (see **Figure 4**).

212
213 2.1.3. Install a manual pressure-reducing valve in the gas tank nozzle. Connect the valve with the
214 gas filling channel at the bottom plate of the visualized vessel by soft pipe (with an inner diameter
215 of 5 mm and a maximal pressure of 30 MPa). Link the vacuum channel and the vacuum pump
216 with the same pipe.

217
218 2.1.4. Fix the back door of the visualized vessel with high-strength bolts. Connect the computer,
219 data acquisition box (DAQ box), and the embedded gas pressure sensor to the back door.

220

2.2. Air tightness test and blank measurement

2.2.1. To acquire the gas pressure data in the visualized vessel, launch the software **DAQ Sensor-16** (or equivalent). On the software, click on **Start**.

2.2.2. Start the vacuum pump. Open the valve V1 (**Figure 2**) and close V2, V3, and V4 (**Figure 2**). Vacuum the visualized vessel chamber. Turn off V1 and vacuum-pump it until it is under vacuum.

2.2.3. Open V2 and the gas tank (with helium). Use the manual pressure-reducing valve to adjust the outlet pressure of the gas tank to approximate 2 MPa (relative pressure).

2.2.4. Carefully observe the gas pressure curve displayed on **DAQ Sensor-16**. When it is about 2 MPa, turn off V2 and the gas tank.

NOTE: After 24 h, if the reduction of the gas pressure is less than 5%, the sealability of the visualized vessel is good.

2.2.5. To measure the friction force of the loading piston moving downward, launch the software **WinWdw** to control the electro-hydraulic servo universal testing machine.

2.2.6. In the software, click on **Force Range** to set the maximum force to 5 kN and click on **Reset** to clear the displacement value. Left-click on the option **Displacement Loading Rate**. Set the moving ratio at 1 mm/min; then, click on **Start**.

2.2.7. When the displacement displayed on **WinWdw** is approximately 5 mm, click on **Stop**. Left-click on **Data Save** to save the force-displacement curve.

2.2.8. Open V4 and discharge helium into air. Disassemble the back door of the visualized vessel and close V4.

CAUTION: The door and windows should be open for ventilation during the gas release due to the possible suffocation hazard.

2.3. Uniaxial compression experiment

2.3.1. Measure the height (h) and diameter (d) of the briquette with a Vernier caliper (with a precision of 0.02 mm). Weigh the mass (m) of the briquette with electronic scales (with a precision of 0.01 g). Calculate its apparent density (ρ) with the following equation.

$$\rho = \frac{4m}{\pi d^2 h}$$

2.3.2. Install the chain roller of the circumferential deformation test apparatus around the middle position of the briquette (**Figure 5**, #1) and fix the clamp holder (**Figure 5**, #2). Connect the sensor (**Figure 5**, #3) with the DAQ box through the aviation connector in the visualized vessel (**Figure 2**)

and place them under the loading piston.

NOTE: To ensure the accuracy of the data acquisition, adjust the chain roller and the top surface of the sample so that they are parallel to the loading piston.

2.3.3. Launch **WinWdw** to control the universal testing machine. In the software, left-click on the option **Displacement Loading Rate**. Set the moving ratio at 10 mm/min. Press the **Down** button on the remote controller of the universal testing machine until the distance left between the piston and the sample is ~1–2 mm. Then, assemble the back door of the visualized vessel.

2.3.4. Repeat steps 2.2.1–2.2.2. Open V3 and the gas tank (CO₂, purity = 99.99%). Use the manual pressure-reducing valve to adjust the outlet pressure of the gas tank to a certain value.

2.3.5. Carefully observe the gas pressure curve displayed in **DAQ Sensor-16**. When it gets close enough to the target value, close V3 and the gas tank (CO₂).

NOTE: When the gas pressure curve remains stable, the briquette has reached its adsorption and desorption dynamic equilibrium state. Generally, it takes ~6–8 h for the briquette to fully adsorb. In this test, the adsorption time is set at 24 h.

2.3.6. After 24 h, place the camera with a tripod beside the window of the visualized vessel. Adjust the height and angle to ensure that the image of the sample is shown in the center of the camera screen.

2.3.7. Start the software **SDU deformation acquisition V2.0** (or equivalent) to monitor the circumferential deformation of the briquette. Click on **Start**.

2.3.8. On **WinWdw**, click on **New Sample** and type in the height and diameter of the briquette, click on **Sectional Area**, and then click on **Confirm**. Click on **Force Range** to set the maximum force to 5 kN, and click on **Reset** to clear the displacement value.

2.3.9. Left-click on the option **Displacement Loading Rate** and set the moving ratio at 1 mm/min. Click on **Start** to compress the sample. At the same time, press the **Start** button on the camera to begin video recording.

2.3.10. When the sample totally fails, click on **Stop** and **Data Save**, in that order, in both **WinWdw** and **SDU deformation acquisition V2.0**. Press the **Start** button again on the camera to stop video recording.

2.3.11. Repeat step 2.2.8 to release CO₂ in the vessel chamber. Disconnect the aviation connectors for the gas pressure sensor and circumferential deformation test apparatus.

2.3.12. Left-click on the option **Displacement Loading Rate** on **WinWdw**. Set the moving ratio at 10 mm/min. Press the **Up** button on the remote controller of the universal testing machine.

When the loading piston of the vessel is around ~2–3 mm above the briquette, take the briquette out and remove it from the chain roller.

2.3.13. Dismantle the connecting tool between the pistons. Clean the visualized vessel with a vacuum cleaner.

2.4. Completion

2.4.1. Based on the stress-axial strain curve and circumferential strain curve obtained from **WinWdw** and **SDU deformation acquisition V2.0**, calculate the volume strain of the sample with the following equation.

$$\varepsilon_V = \varepsilon_1 + 2\varepsilon_2$$

Here, ε_V = volume strain; ε_1 = axial strain; ε_2 = circumferential strain.

2.4.2. Obtain the peak strength from the stress-axial strain curve. The strength reduction rate is calculated as follows.

$$a = \left(1 - \frac{\sigma_{\max}}{\sigma_0}\right) \times 100\%$$

Here, a = strength reduction rate; σ_{\max} = peak strength of the sample under a different pressure of CO₂; σ_0 = peak strength of the sample in atmospheric air.

2.4.3. Calculate the elastic modulus using the linear stage in the stress-axial strain curve according to the following equation.

$$E = \frac{\Delta\sigma}{\Delta\varepsilon}$$

Here, E = elastic modulus of the sample; $\Delta\sigma$ = stress increment of linear the stage (in megapascal); $\Delta\varepsilon$ = strain increment of the linear stage. Calculate the elastic modulus reduction rate as follows.

$$b = \left(1 - \frac{E}{E_0}\right) \times 100\%$$

Here, b = elastic modulus reduction rate, E = elastic modulus of the sample under a different pressure of CO₂; E_0 = elastic modulus of the sample in atmospheric air.

2.4.4. Select sample photos during the test and statistics fracture covering area using a program (e.g., written in MATLAB) according to the box-counting dimension method.

$$\lg N(\delta) = \lg k + D \lg \delta$$

Here, $N(\delta)$ = grid number to cover the fracture area at the square grid side length of δ ; k = a constant; D = fractal dimension; δ = side length of the square grid. The minimum grid size equals the pixel size in this test.

2.4.4.1. Calculate the correlation coefficient according to the following equation.

$$R^2 = \frac{COV(\lg N(\delta), \lg \delta)}{\sqrt{Var[\lg N(\delta)]Var[\lg \delta]}}$$

Here, R^2 = correlation coefficient; $COV(\lg N(\delta), \lg \delta)$ = covariance of $\lg N(\delta)$ and $\lg \delta$; $Var[\lg N(\delta)]$ = variance of $\lg N(\delta)$; $Var[\lg \delta]$ = variance of $\lg \delta$.

REPRESENTATIVE RESULTS:

The average mass of the briquette sample was 230 g. Depending on the industrial analysis, the briquette exhibited a moisture content of 4.52% and an ash content of 15.52%. Furthermore, the volatile content was approximately 31.24%. As the sodium humate was extracted from the coal, the components of the briquette were similar to raw coal. The physical characteristics are displayed in **Table 2**.

The comparison of the mechanical properties between raw coal and briquette are shown in **Table 3**, and the isothermal adsorption test proved their similar capacity for gas adsorption (**Figure 6**). The strength of the briquette samples used in the test had some fluctuation (**Figure 7**). However, compared with the strength reduction induced by CO_2 adsorption, it was rather slight and had little influence on the analysis of the experimental results.

When under different CO_2 pressures, the stress-axial strain curves showed obvious compaction, elastic, and plastic deformation phases (**Figure 8a**). In the post-peak state, the briquette gradually failed, with a surface crack expanding and connecting. A volume expansion was observed from the stress-volume strain curves, and it increased with the CO_2 pressure becoming higher (**Figure 8a**). The CO_2 sorption caused damage to the coal body, which directly reduced its uniaxial compressive strength. The peak strengths of the briquette were 1.011 MPa, 0.841 MPa, 0.737 MPa, 0.659 MPa, 0.611 MPa, and 0.523 MPa under CO_2 pressure from 0 MPa, 0.4 MPa, 0.8 MPa, 1.2 MPa, and 1.6 MPa to 2.0 MPa. As the CO_2 pressure increased, the peak strength of the coal sample decreased, where it showed a nonlinear relationship (**Figure 8b**). In addition, the elastic moduli were 66.974 MPa, 48.271 MPa, 42.234 MPa, 36.434 MPa, 32.509 MPa, and 29.643 MPa, in that order, of CO_2 pressure from 0 to 2.0 MPa. The results indicate that the elastic modulus decreased under the CO_2 saturated condition and that the relationship between the elastic modulus decrease and the gas pressure was nonlinear, which was similar to that of peak strength (**Figure 8c**).

The images obtained through the camera evince the fractures' evolution on the sample's surface under different CO_2 pressures. To distinguish different fractures, all photos were transferred into

binary images and several colors were used to indicate areas covered by fractures (**Figure 9a**). The box-counting dimension method was adopted to describe the feature of fractures in failure state ($\frac{\sigma}{\sigma_{max}} = 0.1$; here, σ = stress of the sample in post-peak state; σ_{max} = peak strength of the sample) under different CO₂ pressures. The correlation coefficients between the box number ($\lg N(\delta)$) and the side length ($\lg \delta$) were all more than 0.95 (**Figure 9b**), which verifies the obvious fractal characteristics of fractures. The fractal dimensions (D) were 1.3495, 1.3711, 1.4336, 1.4637, 1.5175, and 1.5191 for the briquette under 0 MPa, 0.4 MPa, 0.8 MPa, 1.2 MPa, 1.6 MPa, and 2.0 MPa CO₂, respectively. The values of the fractal dimension were proportional to those of CO₂ pressure, and their trend indicated similarity to that of the degree of damage to the coal body.

FIGURE AND TABLE LEGENDS:

Figure 1: Experimental setup of the visualized and constant-volume gas-solid coupling test system. The figure demonstrates the setup of a uniaxial compression experiment of CO₂-bearing coal. (A) Visualized loading vessel. (B) Gas filling module. (C) Axial loading module. (D) Data acquisition module.

Figure 2: The visualized loading vessel. Schematic drawings of the vessel are shown above. While the sample (height = 100 mm, diameter = 50 mm) lay within the vessel, axial pressure was applied by the independent universal testing machine through the loading piston, and high-pressure gas was injected from the gas tank through the soft pipe and the filling channel. When the sample was warped by the thermal contractible plastic sleeve, the confining pressure was also provided by high-pressure helium. The two adjusting cylinder pistons and the loading one of the visualized vessel moved simultaneously, where the movement-induced volume change was offset because of their same sectional area. This structure kept the vessel volume constant and eliminated the antforce applied on the loading piston from gas. The sample could be monitored with a camera through the windows on three sides. The aviation connector was set in the vessel for a lead-out wire connection.

Figure 3: Shaping tools required to cold-press the standard briquette. 3D schematic views of how the briquette was pressed (29.4 KN for 15 min). The sample lay in the inner hole of the tool components, and its height and diameter were 100 mm and 50 mm, respectively.

Figure 4: Tool required to connect the loading pistons. 3D schematic views of the fixing tool between the piston of the electro-hydraulic servo tester and that of the visualized vessel.

Figure 5: Standard test apparatus for the circumferential deformation of rock samples. Schematic and physical representation of the circumferential deformation acquisition used in the protocol. By measuring the angular displacement induced by sample circumferential deformation, the circumferential strain was obtained. This apparatus can stably operate in high-pressure gas and hydraulic oil.

Figure 6: Comparison of the adsorption capacity between raw coal and briquette. The panel shows the methane isothermal adsorption data using raw coal and briquette according to per standard GB/T19560-2008.

Figure 7: The full stress-strain curves generated from the test system using briquette. A uniaxial compression test was conducted using three briquette samples without CO₂ filling, and results show that briquette has a stable uniaxial compression strength (1.0 MPa).

Figure 8: Uniaxial compression experiment of CO₂-bearing coal. (A) Stress-strain curves under different CO₂ pressures. (B) Trend of change in peak strength. (C) Trend of change in elastic modulus. The stress- axial strain curves ($\sigma - \varepsilon_1$), stress-circumferential strain curves ($\sigma - \varepsilon_2$), and stress-volume strain curves ($\sigma - \varepsilon_V$) are shown in panel A. After filling with CO₂, the briquette experienced peak strength and elastic modulus reduction, and the curves in panels B and C indicate a nonlinear relationship between the reduction rate and the gas pressure.

Figure 9: The images of fractures and fractal calculation in failure state ($\frac{\sigma}{\sigma_{max}} = 0.1$). (A) Fracture evolution on briquettes' surfaces, with different colors representing varied fractures. (B) Fractal dimension curves using the box-counting dimension method. Fractures were extracted and the covering area was calculated based on fractal geometry. All correlation coefficients (R^2) under different CO₂ pressures were more than 0.95, which proves the fractal characteristics.

Figure 10: Tools required to apply dynamic load and photo of the test system. 3D view and physical picture of the guide rod and the cylindrical weight for dynamic load applying.

Table 1: Scheme of briquette preparation.

Table 2: The comparison of industrial analysis parameters for briquette and raw coal.

Table 3: The mechanical characteristics of raw coal and briquette.

DISCUSSION:

Considering the danger of high-pressure gas, some critical steps are important during the test. The valves and O rings should be inspected and replaced regularly, and any source of ignition should not be allowed in the laboratory. When using the manual pressure-regulating valve, the experimenter should twist the valve slowly to make the pressure in the visualized vessel increase gradually. Do not disassemble the vessel during the test. When the experiment is finished, the back door of the vessel should be opened after the total release of the high-pressure gas; otherwise, there is a danger of injury. Use a vacuum cleaner to remove all pieces of briquette from the vessel, so as not to affect the quantity of gas adsorption during the next test.

The CO₂-coal coupling experimental method was designed to promote test precision and provide photograph monitoring for gas-bearing coal experiments. The briquette sample possesses several advantages, such as cost-effectiveness, nontoxicity, easy manufacture, stable

performance, and adjustable strength, and its isothermal adsorption curve agrees well with that of raw coal. The model test of coal and gas outburst also proves that briquette can simulate the adsorptive and desorptive behavior of gas-bearing coal^{29,31}. In addition, after five generations of improvement, the experimental apparatus now has high accuracy, precision, stability, and safety, which complies with the standards for the safety of high-pressure experiments. There is no particular requirement for the species of the sample, as long as it is a porous rock, including raw coal and shale rock.

The main limits of the CO₂-coal coupling experimental method are, first, that briquette has a lower strength compared with raw coal, due to its way of formation. The similarity of mechanical properties between the raw coal and the briquette still needs improvement, and related experimental results should be evaluated and validated by raw coal and an in situ test. Second, since the LED lights and aviation connector were set in a visualized vessel, it should not be filled with any flammable gas, such as CH₄. Otherwise, an explosive accident is likely to occur during the gas filling. Fortunately, a noncombustible gas similar to methane can simulate the CH₄-coal interaction and it has been proven as a safe and effective material to apply in coal and gas outburst physical simulation experiments³².

Additionally, the briquette is wrapped by a thermal contractible plastic sleeve for confining the pressure applied during the triaxial compression test, which will evidently degrade the quality of the sample image. When the sample is loaded under a different gas, temperature, and gas pressure, the dynamic index of the refraction needs to be taken into consideration during image capturing. As the pressure difference in the test is relatively low, the index of refraction can be seen as a constant³³.

Apart from the uniaxial and triaxial compression, dynamic load disturbance can be applied during the test to investigate the interaction between the sample and the gas. The guide rod and a 1 kg cylindrical weight are added between the pistons of the universal testing machine and the visualized vessel (**Figure 10**). The pressure sensor is installed on the bottom of the loading piston to acquire the dynamic pressure applied to the sample. During the test, the cylindrical weight, at a certain height, is released in different stress states to study the sample's dynamic failure characteristics.

The sorption-induced damage to the coal body is macroscopically revealed as a reduction of the uniaxial compressive strength and elastic modulus. The higher the sorption pressure is, the greater the coal damage causes, which is a nonlinear relationship. The adsorption process can be described by the Langmuir model³⁴. According to the model equation, $V = \frac{V_m b p}{1 + b p}$ (V = equivalent adsorption volume; V_m , b = constant; p = gas pressure), the adsorption quantity increases as the gas pressure increases. This difference results in the different reduction rates of peak strength of briquette. The coal strength or elastic modulus reduction by CO₂ saturation observed from experimental results have good conformity with previous research^{35,36,37}. In conclusion, there must be a certain relationship between mechanical damage caused by sorption and gas adsorption quantity.

The deformation characteristics of briquette are summarized as the compression/expansion connection of microcracks and the final formation of macroscopic fractures. It is suggested that the fracture evolution of CO₂-bearing coal showed fractal characteristics. The maximum fractal dimension was 1.5191 (2 MPa CO₂) in the test. Considering that raw coal is more heterogeneous than briquette, the value of the fractal dimension may be different for the raw coal test.

Rock is a solid medium, and various external effects will cause damage to it. Due to the uncertainty of crack propagation during the failure process, especially considering the coupling effect of sorption and loading, some traditional rock mechanics research methods manifest obvious limitations. However, the fractal theory provides a new way to describe and study the complex mechanical processes and mechanisms of rock fracture development. Previous studies have made it clear that the fracture evolution of rock materials has fractal features^{38,39,40,41}. However, test research on the fracture evolution of gas-bearing coal is lacking, mainly because of a limitation of the experimental apparatus. The CO₂-coal coupling experimental method provides scientists with a way to capture and extract the surface fracture network of the sample through windows and obtains the fractal dimension in different coupling conditions. The fractal dimension can be used to quantitatively describe the damage degree, fracture development, and section complexity of coal body under the loading status. It can become an evaluation index for structural characteristics and mechanical properties of coal. Therefore, it is of great significance to the evaluation of gas storage capacity and injection influence parameters in the practice of CO₂ geological sequestration.

ACKNOWLEDGMENTS:

This work was supported by the China National Major Scientific Instruments Development Project (Grant No. 51427804) and the Shandong Province National Natural Science Foundation (Grant No. ZR2017MEE023).

DISCLOSURES:

The authors have nothing to disclose.

REFERENCES:

1. Mazzotti, M., Pini, R., Storti, G. Enhanced coalbed methane recovery. *Journal of Supercritical Fluids*. **47** (3), 619-627 (2009).
2. Litynski, J. et al. U.S. Department of Energy's Regional Carbon Sequestration Partnership Program: Overview. *Energy Procedia*. **1** (1), 3959-3967 (2009).
3. Lackner, K. S. A Guide to CO₂ Sequestration. *Science*. **300** (5626), 1677-1678 (2015).
4. Zhou, F. D. et al. A feasibility study of ECBM recovery and CO₂ storage for a producing CBM field in Southeast Qinshui Basin, China. *International Journal of Greenhouse Gas Control*. **19** (19), 26-40 (2013).
5. Zhou, F., Hussain, F., Cinar, Y. Injecting pure N₂ and CO₂ to coal for enhanced coalbed methane: Experimental observations and numerical simulation. *International Journal of Coal Geology*. **116-117** (5), 53-62 (2013).
6. Pini, R., Ottiger, S., Storti, G., Mazzotti, M. Pure and competitive adsorption of CO₂, CH₄ and

564 N₂ on coal for ECBM. *Energy Procedia*. **1** (1), 1705-1710 (2009).

565 7. Nie, B. S., Li, X. C., Cui, Y. J., Lu, H. Q. *Theory and application of gas migration in coal seam*.
566 Science Press. Beijing, China (2014).

567 8. Scott, A. R. Improving coal gas recovery with microbially enhanced coalbed methane. In
568 *Coalbed Methane: Scientific, Environmental and Economic Evaluation*. Edited by Mastalerz, M.,
569 Glikson, M., Golding, S. D., 89-110, Springer. Netherlands (1999).

570 9. Gorucu, F. et al. Effects of matrix shrinkage and swelling on the economics of enhanced-
571 coalbed-methane production and CO₂ sequestration in coal. *Spe Reservoir Evaluation*
572 *Engineering*. **10** (4), 382-392 (2007).

573 10. Liu, S. M., Wang, Y., Harpalani, S. Anisotropy characteristics of coal shrinkage/swelling and its
574 impact on coal permeability evolution with CO₂ injection. *Greenhouse Gases Science &*
575 *Technology*. **6** (5), 615-632 (2016).

576 11. Larsen, J. W. The effects of dissolved CO₂, on coal structure and properties. *International*
577 *Journal of Coal Geology*. **57** (1), 63-70 (2004).

578 12. Mastalerz, M., Gluskoter, H., Rupp, J. Carbon dioxide and methane sorption in high volatile
579 bituminous coals from Indiana, USA. *International Journal of Coal Geology*. **60** (1), 43-55 (2004).

580 13. Li, X. C., Nie, B. S., He, X. Q., Zhang, X., Yang, T. Influence of gas adsorption on coal body.
581 *Journal of China Coal Society*. **36** (12), 2035-2038 (2011).

582 14. Du, Q. H, Liu, X. L., Wang, E. Z. Wang, S. J. Strength Reduction of Coal Pillar after CO₂
583 Sequestration in Abandoned Coal Mines. *Minerals*. **7** (2), 26-41 (2017).

584 15. Zhao, B. et al. Similarity criteria and coal-like material in coal and gas outburst physical
585 simulation. *International Journal of Coal Science and Technology*. **5** (2), 167-178 (2018).

586 16. Xu, J., Ye, G.-b., Li, B.-b., Cao, J., Zhang, M. Experimental study of mechanical and permeability
587 characteristics of moulded coals with different binder ratios. *Rock and Soil Mechanics*. **36** (1),
588 104-110 (2015).

589 17. Barbara, D. et al. Balance of CO₂/CH₄ exchange sorption in a coal briquette. *Fuel Processing*
590 *Technology*. **106** (2), 95-101 (2013).

591 18. Benk, A., Coban, A. Molasses and air blown coal tar pitch binders for the production of
592 metallurgical quality formed coke from anthracite fines or coke breeze. *Fuel Processing*
593 *Technology*. **92** (5), 1078-1086 (2011).

594 19. Zhao, H, B., Yin, G. Z. Study of acoustic emission characteristics and damage equation of coal
595 containing gas. *Rock and Soil Mechanics*. **32** (3), 667-671 (2011).

596 20. Cao, S. G., Li, Y., Guo, P., Bai, Y. J., Liu, Y. B. Comparative research on permeability
597 characteristics in complete stress-strain process of briquette and coal samples. *Chinese Journal*
598 *of Rock Mechanics and Engineering*. **29** (5), 899-906 (2010).

599 21. Wang, H. P. et al. Development of a similar material for methane-bearing coal and its
600 application to outburst experiment. *Rock and Soil Mechanics*. **36** (6), 1676-1682 (2015).

601 22. Ulusay, R. *The ISRM Suggested Methods for Rock Characterization, Testing and Monitoring:*
602 *2007-2014*. Springer International Publishing. Switzerland (2015).

603 23. Ranathunga, A. S., Perera, M. S. A., Ranjith, P. G. Influence of CO₂ adsorption on the strength
604 and elastic modulus of low rank Australian coal under confining pressure. *International Journal*
605 *of Coal Geology*. **167**, 148-156 (2016).

606 24. Ranjith, P. G., Perera, M. S. A. Effects of cleat performance on strength reduction of coal in
607 CO₂, sequestration. *Energy*. **45** (1), 1069-1075 (2012).

25. Masoudian, M. S., Airey, D. W., El-Zein, A. Experimental investigations on the effect of CO₂, on mechanics of coal. *International Journal of Coal Geology*. **128-129** (3), 12-23 (2014).
26. Wang, S. G., Elsworth, D., Liu, J. S. Rapid decompression and desorption induced energetic failure in coal. *Journal of Rock Mechanics and Geotechnical Engineering*. **7** (3), 345-350 (2015).
27. Hadi Mosleh, M., Turner, M., Sedighi, M., Vardon, P. J. Carbon dioxide flow and interactions in a high rank coal: Permeability evolution and reversibility of reactive processes. *International Journal of Greenhouse Gas Control*. **70**, 57-67 (2018).
28. Abhijit, M., Harpalani, S., Liu, S. M. Laboratory measurement and modeling of coal permeability with continued methane production: Part 1 – Laboratory results. *Fuel*. **94** (1), 110-116 (2012).
29. Li, Q. C. et al. Development and application of a gas-solid coupling test system in the visualized and constant volume loading state. *Journal of China University of Mining & Technology*. **47** (1), 104-112 (2018).
30. Allen, T. *Particle Size Measure*. China Architecture & Building Press. Beijing, China (1984).
31. Wang, H. P. et al. Coal and gas outburst simulation system based on CRISO model. *Chinese Journal of Rock Mechanics and Engineering*. **34** (11), 2301-2308 (2015).
32. Zhang, Q. H. et al. Exploration of similar gas like methane in physical simulation test of coal and gas outburst. *Rock and Soil Mechanics*. **38** (2), 479-486 (2017).
33. Xia, G. Z. *Study on density and refractive index of near-critical fluid*. Master's degree thesis. Huazhong University of Science and Technology (2009).
34. Ruppel, T. C., Grein, C. T., Bienstock, D. Adsorption of methane on dry coal at elevated pressure. *Fuel*. **53** (3), 152-162 (1974).
35. Ranjith, P. G., Jasinge, D., Choi, S. K., Mehic, M., Shannon, B. The effect of CO₂ saturation on mechanical properties of Australian black coal using acoustic emission. *Fuel*. **89** (8), 2110-2117 (2010).
36. Viete, D. R., Ranjith, P. G. The effect of CO₂, on the geomechanical and permeability behaviour of brown coal: Implications for coal seam CO₂ sequestration. *International Journal of Coal Geology*. **66** (3), 204-216 (2006).
37. Jiang, Y. D., Zhu, J., Zhao, Y. X., Liu, J. H., Wang, H. W. Constitutive equations of coal containing methane based on mixture theory. *Journal of China Coal Society*. **32** (11), 1132-1137 (2007).
38. Xie, H. P., Gao, F., Zhou, H. W., Zuo, J. P. Fractal fracture and fragmentation in rocks. *Journal of Seismology*. **23** (4), 1-9 (2003).
39. Miao, T. J., Yu, B. M., Duan, Y. G., Fang, Q. T. A fractal analysis of permeability for fractured rocks. *International Journal of Heat & Mass Transfer*. **81** (81), 75-80 (2015).
40. Liu, R. C., Jiang, Y. J., Li, B., Wang, X. S. A fractal model for characterizing fluid flow in fractured rock masses based on randomly distributed rock fracture networks. *Computers & Geotechnics*. **65**, 45-55 (2015).
41. Pan, J. N. et al. Micro-pores and fractures of coals analysed by field emission scanning electron microscopy and fractal theory. *Fuel*. **164**, 277-285 (2016).

Figure 1

[Click here to access/download;Figure;Figure 1.eps](#)

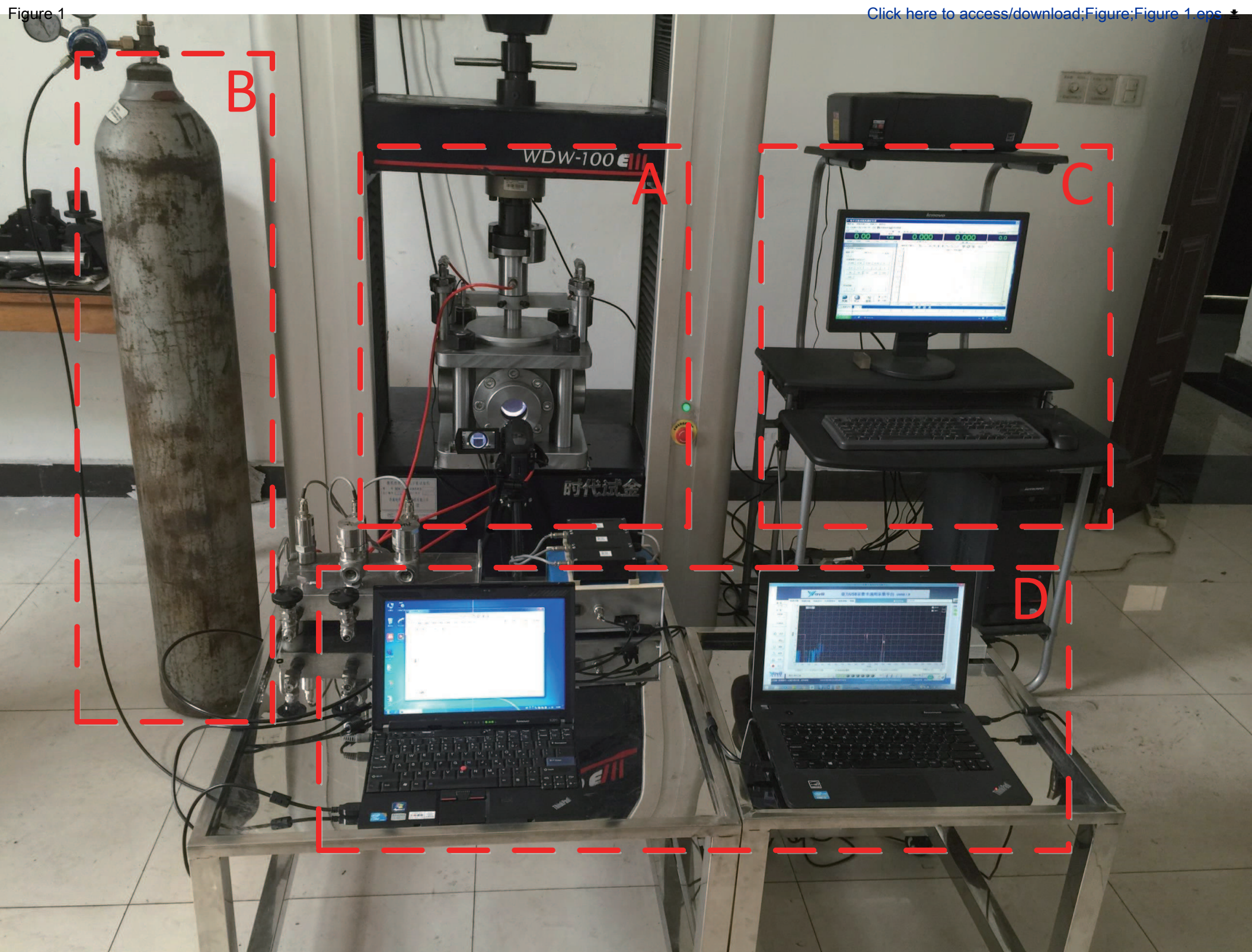


Figure 2

[Click here to access/download;Figure;Figure 2.eps](#)

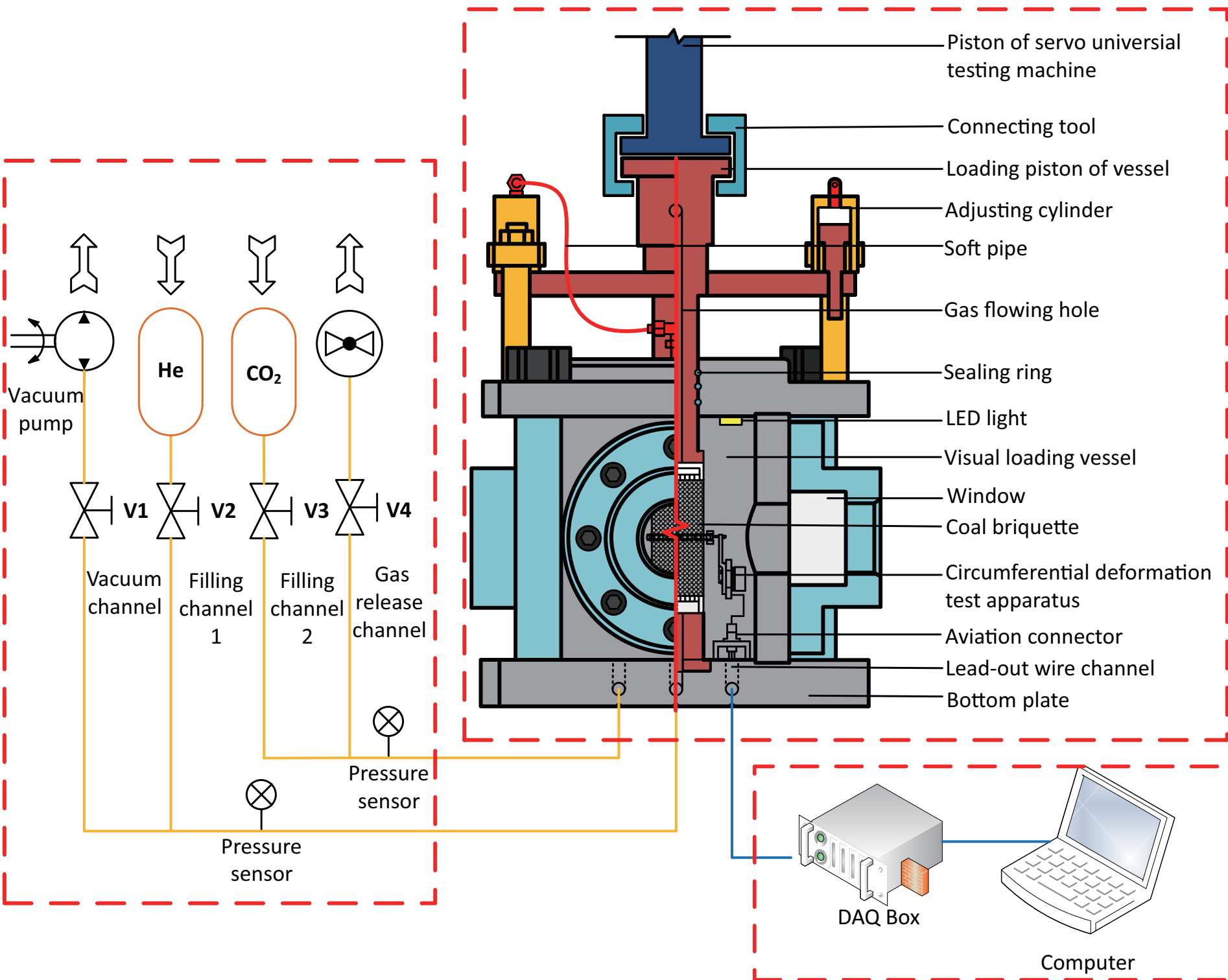


Figure 3

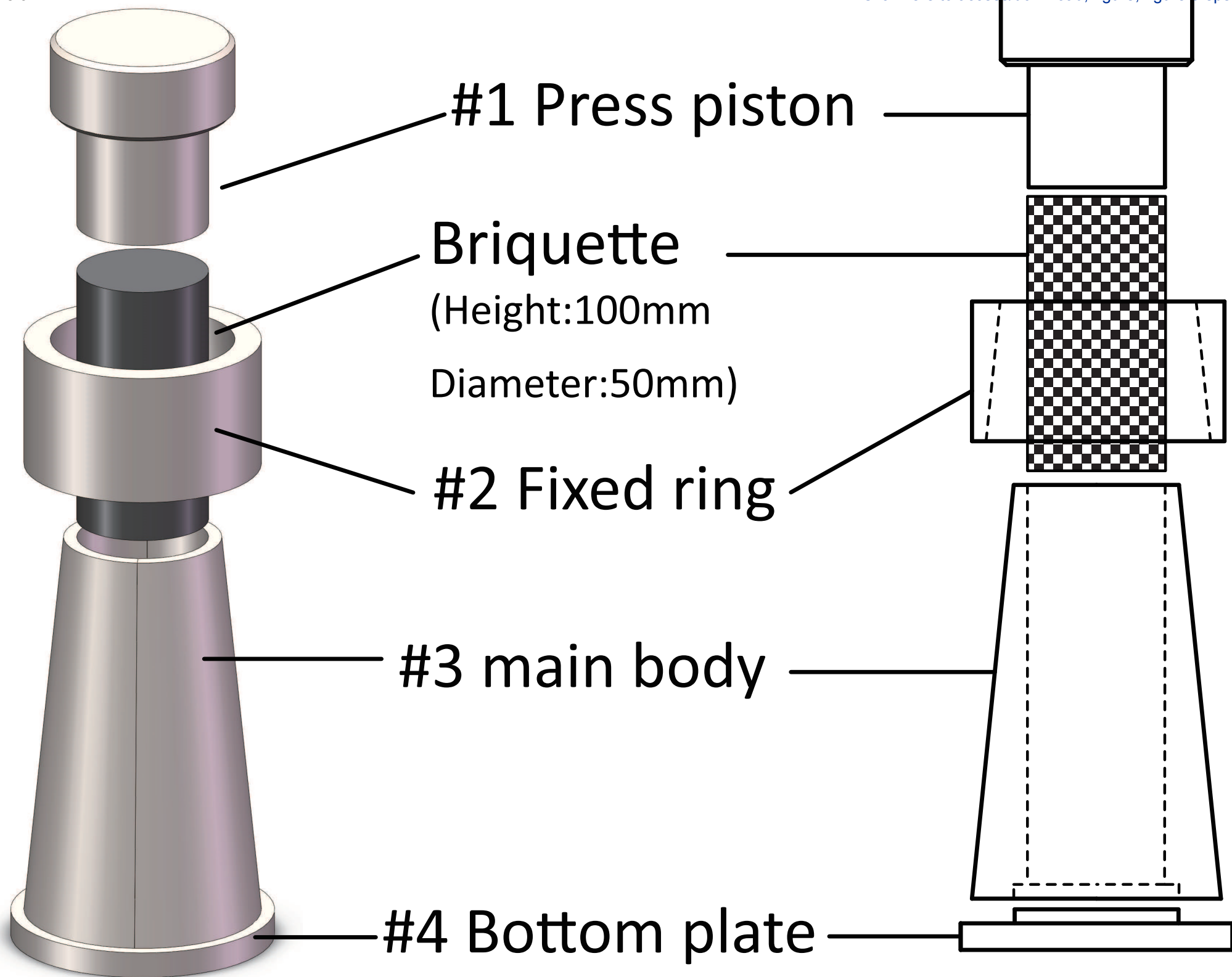
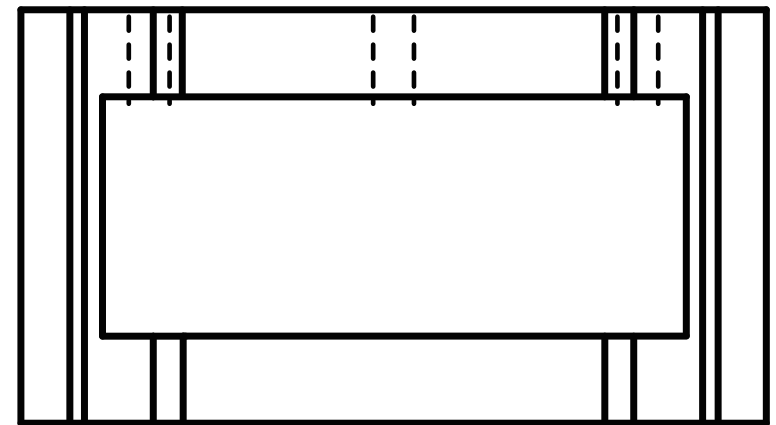
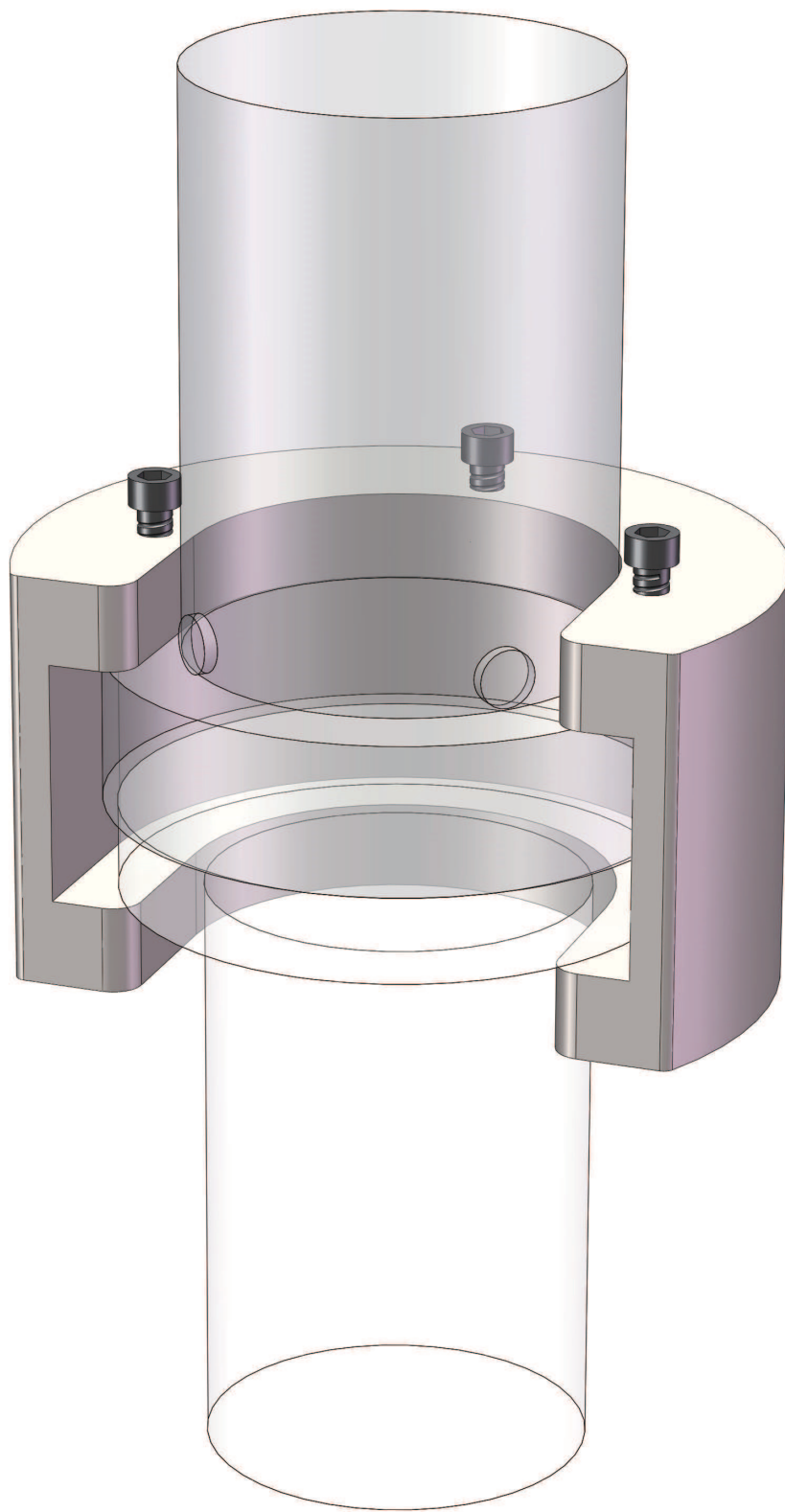
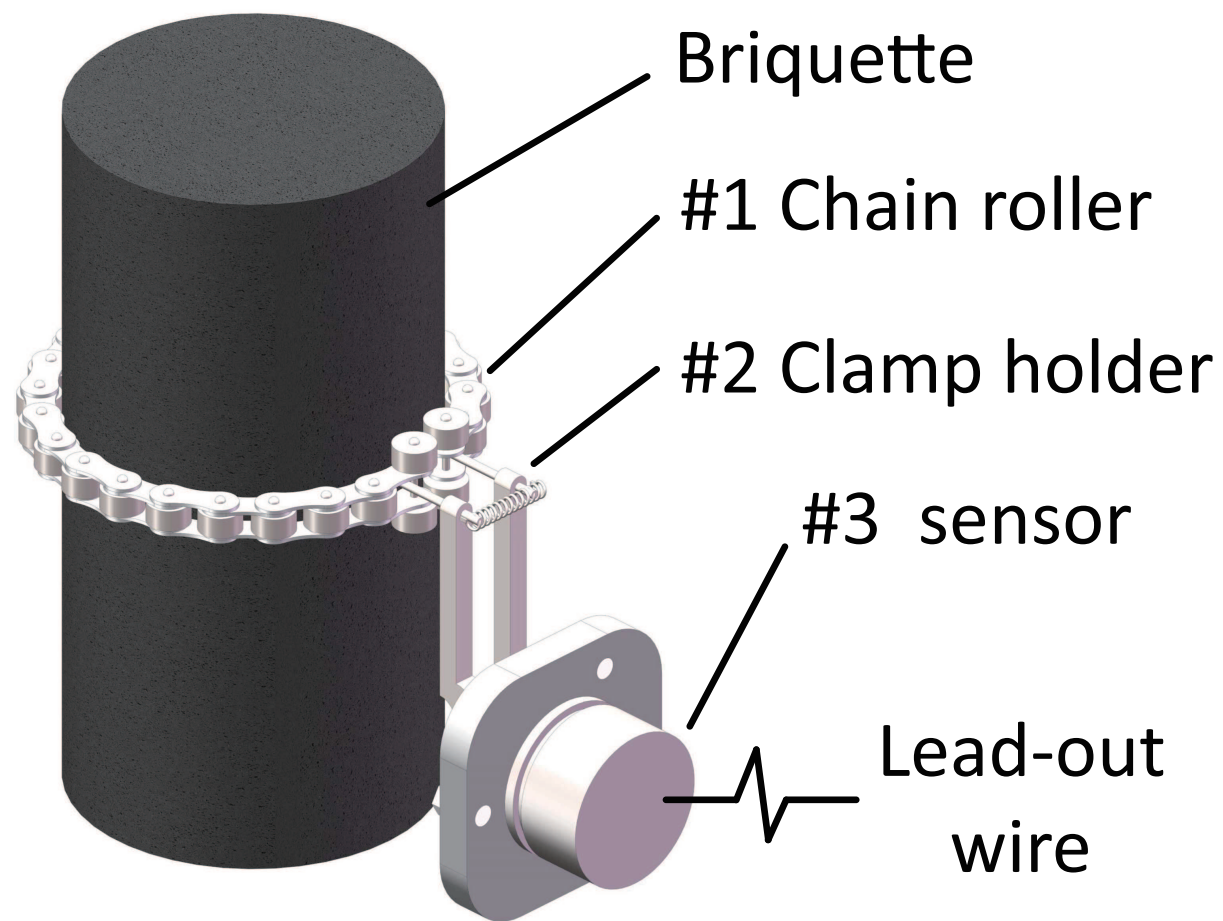


Figure 4



Side view



Physical picture

Figure 6

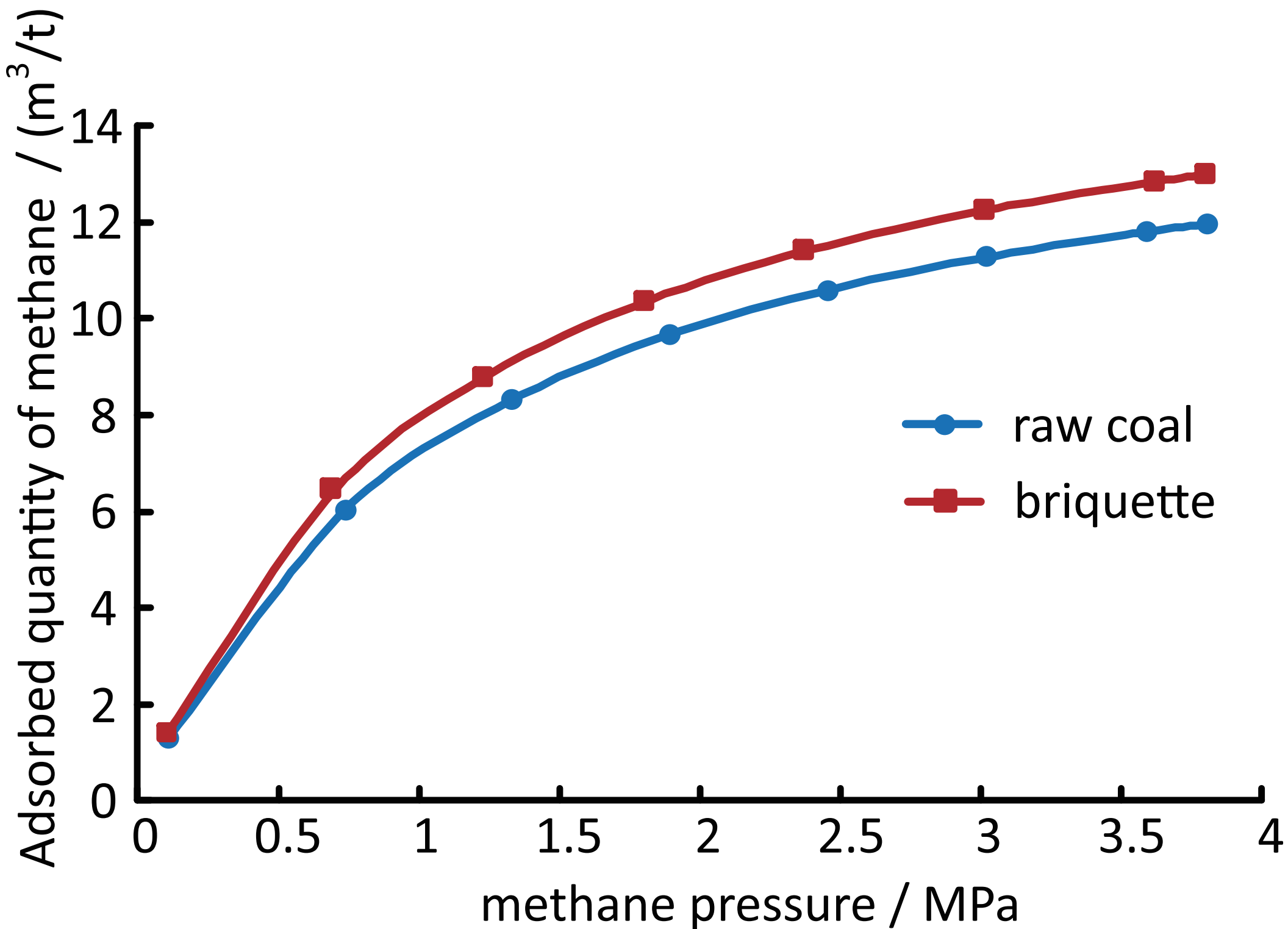
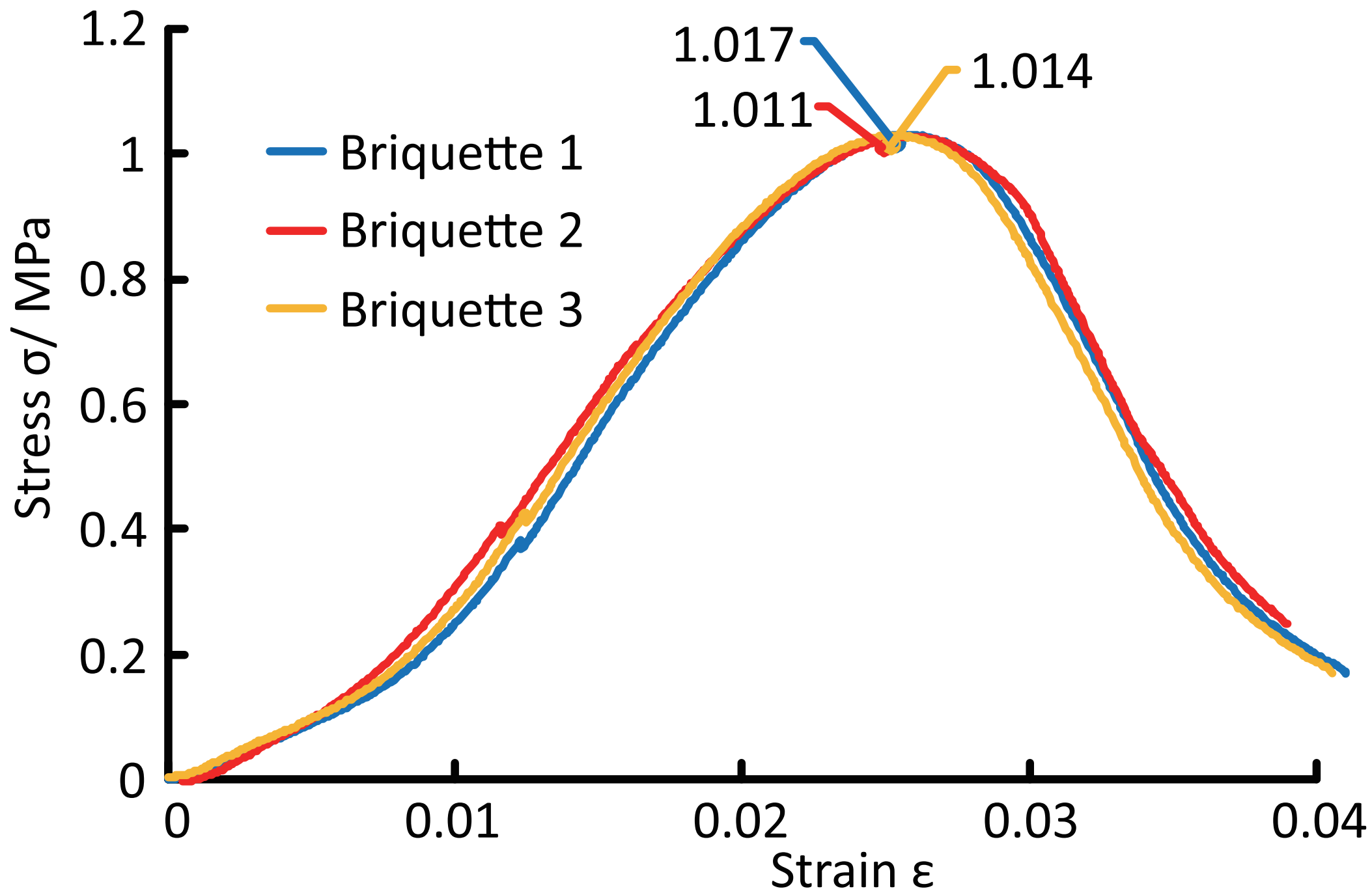
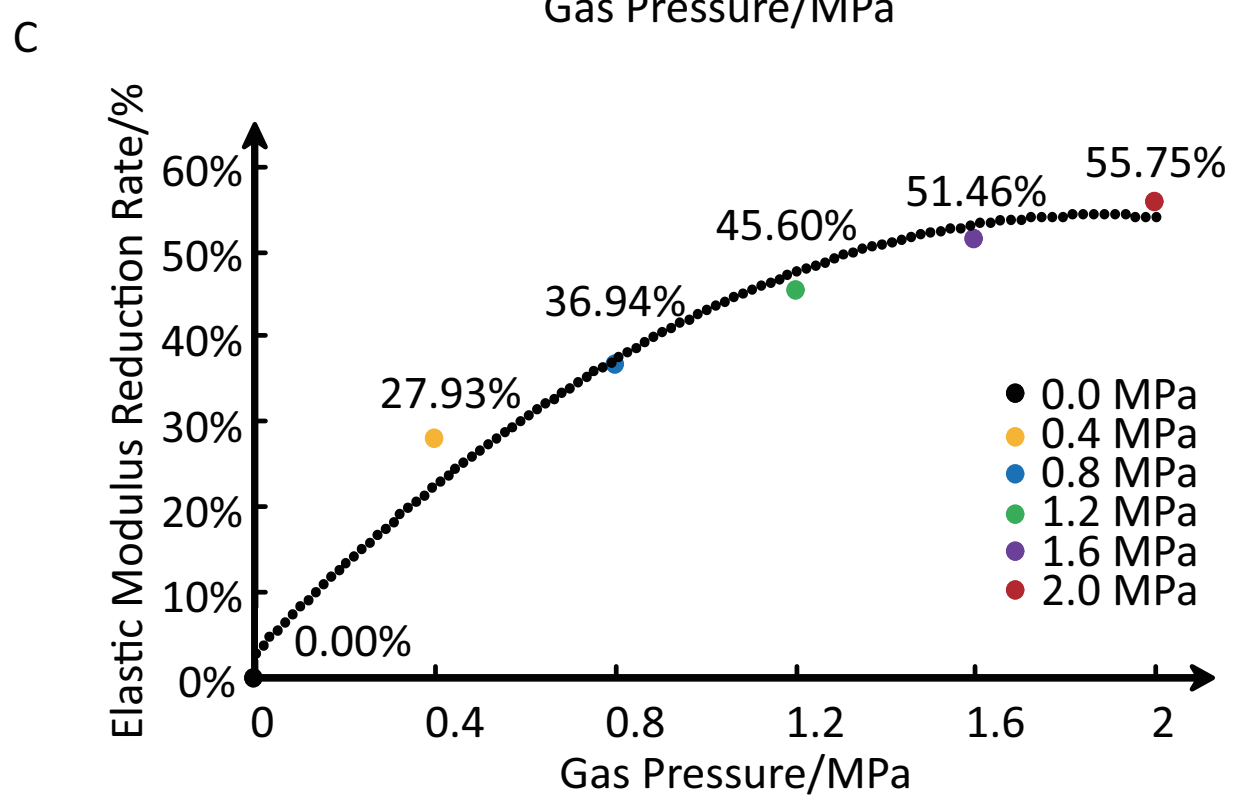
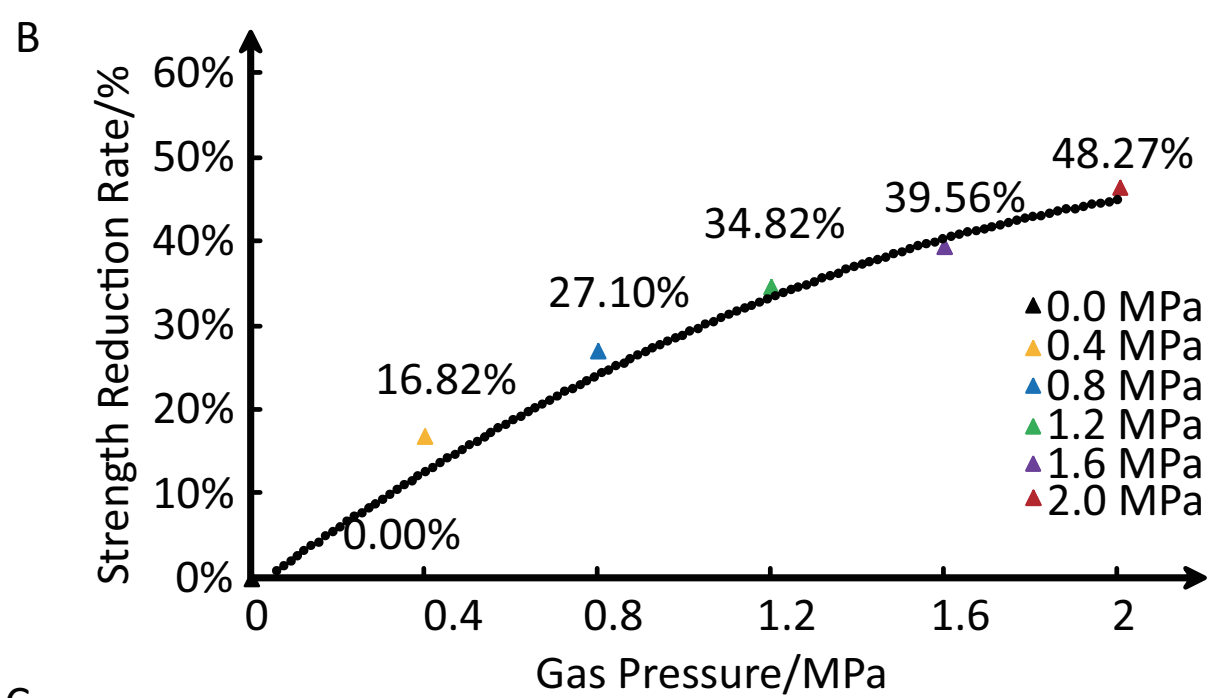
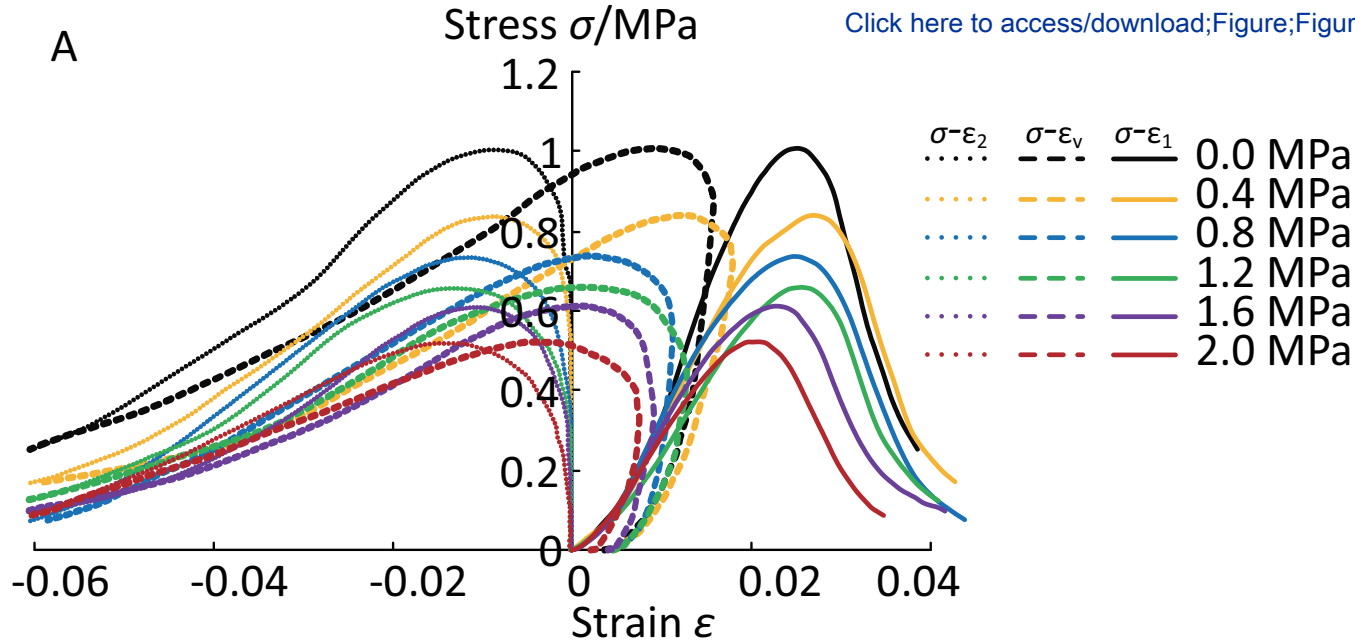
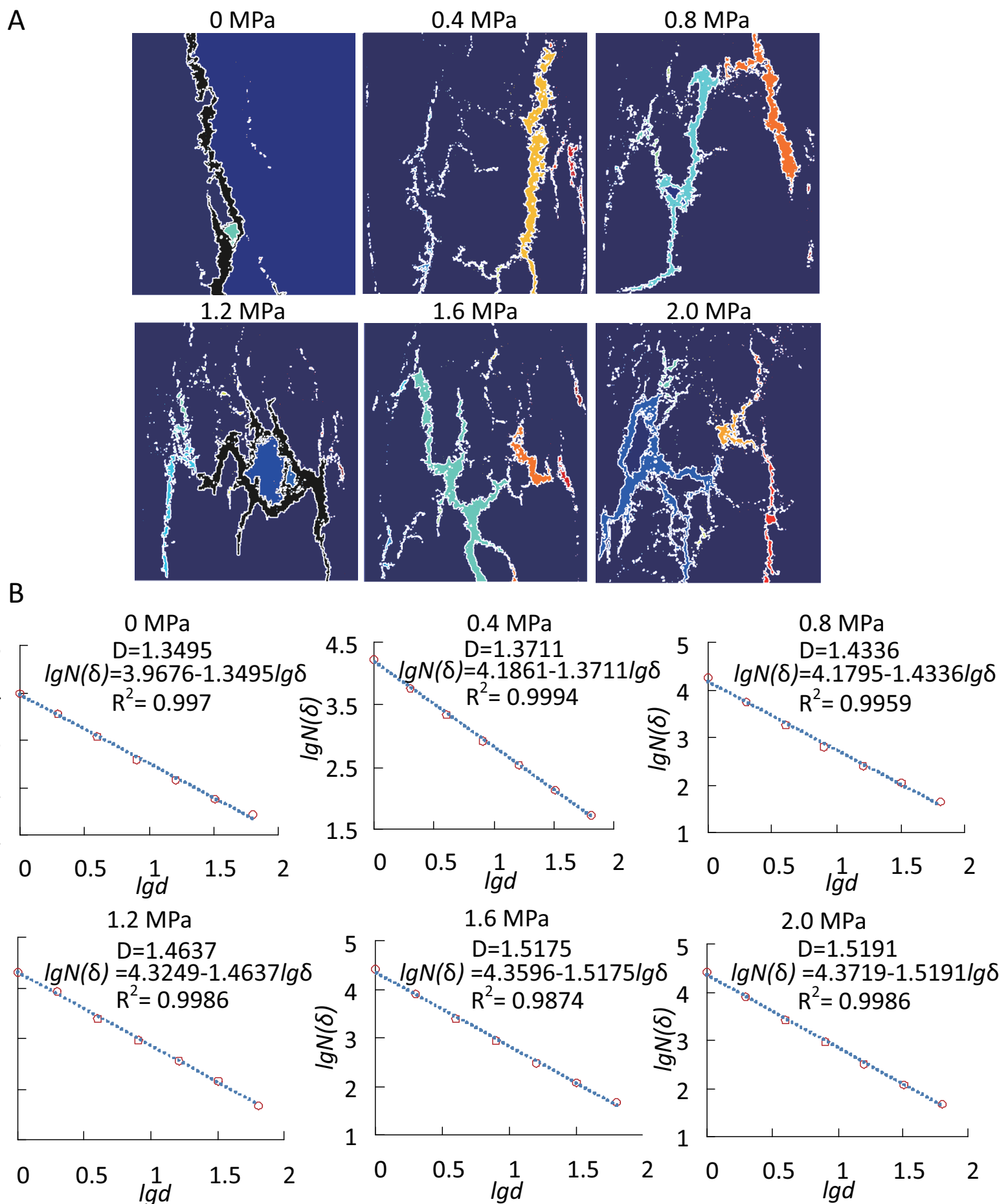
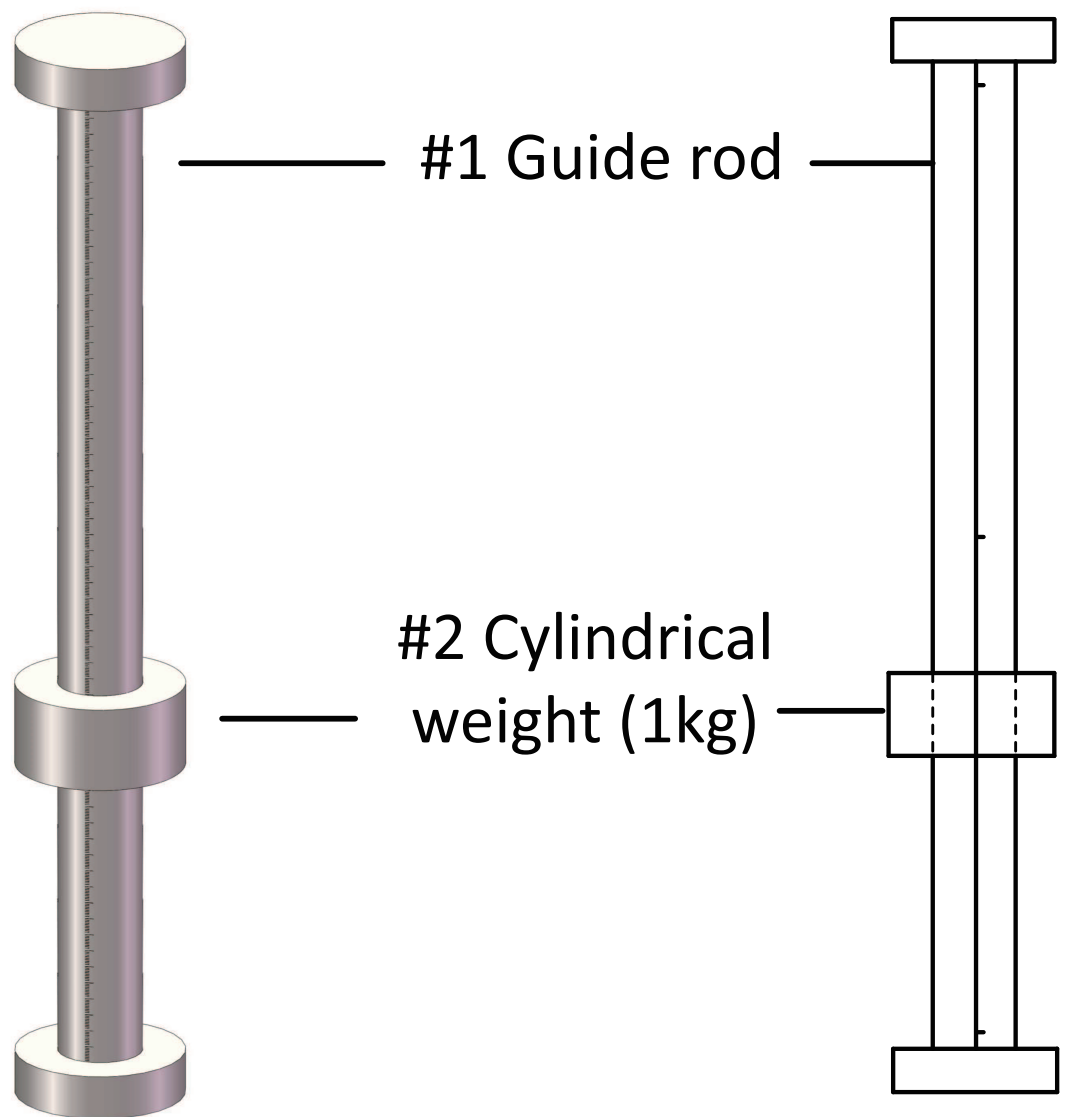


Figure 7

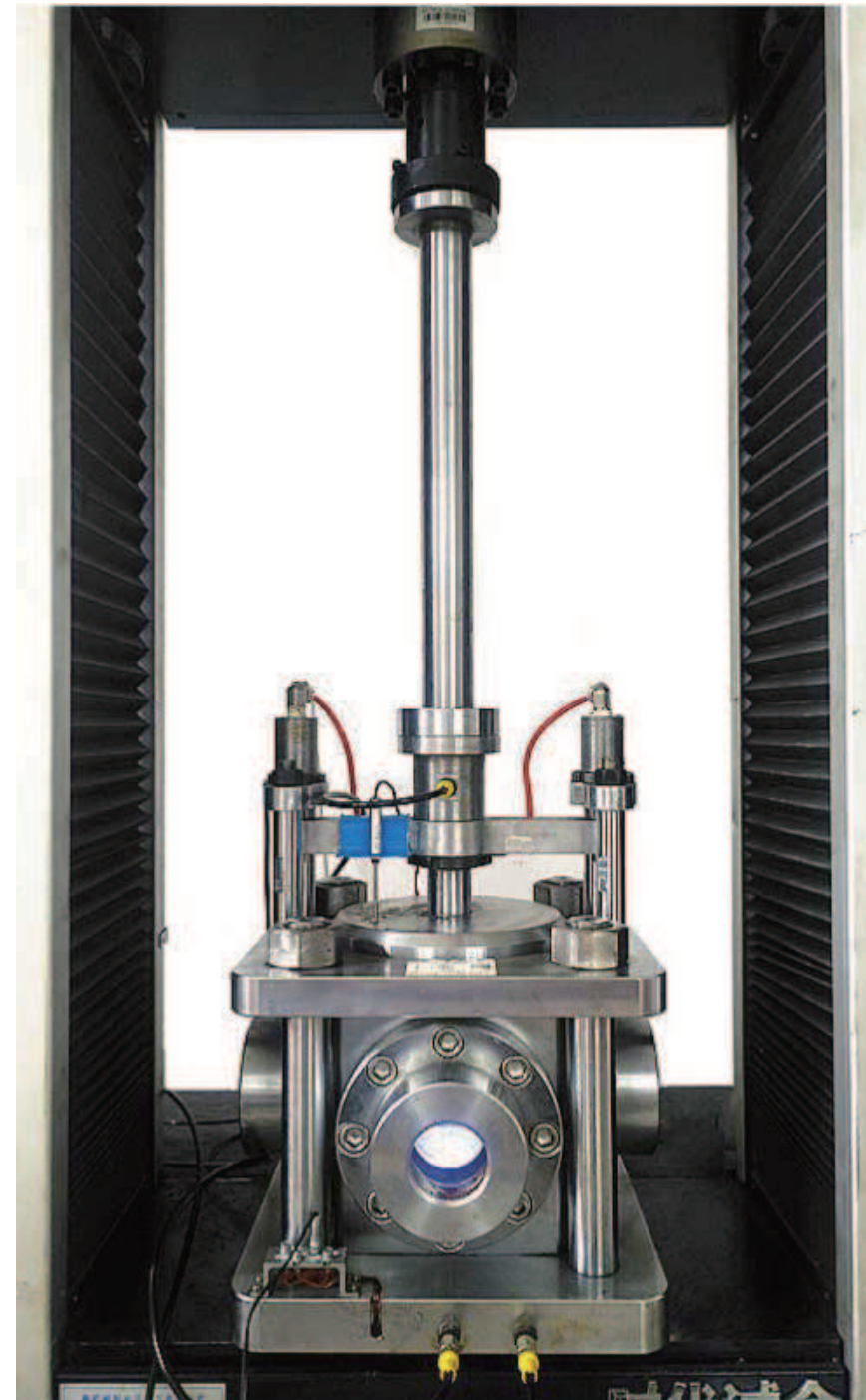








Side view



Physical picture

NO.	Coal grain Composition (0~1 mm:1~3 mm)	Concentration of solidum humate solution/ %	Raito (coal powder: ceme nt)	Mass/ g	Molding Pressure / MPa	Time / min	Peak Strength / MPa
1	0.76:0.24	1	0.92:0.08	250	15	15	0.5
2		4					1
3		7					1.5
4		12					2

sample	apparent density (g/cm3)	Porosity (%)	Moisture content (%)	Ash content (%)	Volatile content (%)	Maximum vitrinite reflectance (%)
Briquette	1.17	15	4.52	15.52	31.24	0.82
Raw coal	1.4	3.45	4.09	15.36	31.17	0.85

Sample	Uniaxial compressive strength (MPa)	Elastic modulus (Gpa)	Tensile strength (MPa)	Internal friction angle (°)	Cohesion (MPa)	Pission ratio
raw coal	25.23	4.529	2.30	30	0.800	0.25
briquette	1.011	0.067	0.11	29	0.117	0.25

Name of Material/ Equipment	Company	Catalog Number	Comments/Description
3Y-Leica MPV-SP photometer microphotometric system	Leica, Germa ny	M090063016	Used for vitrinite reflectance measurement
Automatic isotherm adsorption instrument	BeiShiDe Instrument Technology (Beijing)CO., Ltd.	3H-2000PH	Isothermal adsorption test
Electro hydraulic servo universal testing machine	Jinan Shidaishijin testing machine CO.,Ltd	WDW-100EIII	Used to provide axial pressure
Gas pressure sensor	Beijing Star Sensor Technology CO.,LTD	CYYZ11	Gas pressure monitoring
Gas tank(carbon dioxide/helium)	Heifei Henglong Gas.,Ltd		Gas resource
high-speed camera	Sony corporation	FDR-AX30	Image monitoring
Incubator	Yuyao YuanDong Digital Instrument Factory	XGQ-2000	Briquette drying
jaw crusher	Hebi Tianke Instrument CO.,Ltd	EP-2	Coal grinding

Manual pressure reducing valve	Shanghai Saergen Instrument CO.,Ltd	R41	Outlet gas pressure adjustment
Proximate Analyzer	Changsha Kaiyuan Instrument CO.,Ltd	5E-MAG6700	Coal industrial analysis
Resistance strain gauge	Jinan Sigmar Technology CO.,LTD	ASMB3-16/8	Poisson ratio measurement
Sieve shaker (6,16mesh)	Hebi Tianguan Instrument CO.,Ltd	GZS-300	Coal powder shelter
Soft pipe	Jinan Quanxing High pressure pipe CO.,Ltd		Inner diameter=5 mm maximal pressure=30 MPa
Standard rock sample circumferential deformation test apparatus	Huainan Qingda Machinery CO.,Ltd		Circumferential deformation acquisition
Strain controlled direct shear apparatus	Beijing Aerospace Huayu Test Instrument CO.,LTD	ZJ-4A	Tensile strength, cohesion, internal friction angle measurement
Vaccum pump	Fujiwara,Japan	750D	Used to vaccumize the vessel

Valve	Jiangsu Subei Valve Co.,Ltd	S4 NS-MG16-MF1	Gas seal
Visual loading vessel	Huainan Qingda Machinery CO.,Ltd		Instrument for sample loading and real-time monitoring

ARTICLE AND VIDEO LICENSE AGREEMENT

Title of Article:

Uniaxial Compression Experiment of CO₂-bearing Coal Using the Visula and Constant Volume Gas-solid Coupling Test System

Author(s):

Weitao Hou, Wanghan Peng, Wei Wang, Zhongzhong Liu, Qingchuan Li

Item 1: The Author elects to have the Materials be made available (as described at <http://www.jove.com/publish>) via:

☒ Standard Access

☐ Open Access

Item 2: Please select one of the following items:

☒ The Author is **NOT** a United States government employee.

☐ The Author is a United States government employee and the Materials were prepared in the course of his or her duties as a United States government employee.

☐ The Author is a United States government employee but the Materials were NOT prepared in the course of his or her duties as a United States government employee.

ARTICLE AND VIDEO LICENSE AGREEMENT

1. **Defined Terms.** As used in this Article and Video License Agreement, the following terms shall have the following meanings: **"Agreement"** means this Article and Video License Agreement; **"Article"** means the article specified on the last page of this Agreement, including any associated materials such as texts, figures, tables, artwork, abstracts, or summaries contained therein; **"Author"** means the author who is a signatory to this Agreement; **"Collective Work"** means a work, such as a periodical issue, anthology or encyclopedia, in which the Materials in their entirety in unmodified form, along with a number of other contributions, constituting separate and independent works in themselves, are assembled into a collective whole; **"CRC License"** means the Creative Commons Attribution-Non Commercial-No Derivs 3.0 Unported Agreement, the terms and conditions of which can be found at: <http://creativecommons.org/licenses/by-nc-nd/3.0/legalcode>; **"Derivative Work"** means a work based upon the Materials or upon the Materials and other pre-existing works, such as a translation, musical arrangement, dramatization, fictionalization, motion picture version, sound recording, art reproduction, abridgment, condensation, or any other form in which the Materials may be recast, transformed, or adapted; **"Institution"** means the institution, listed on the last page of this Agreement, by which the Author was employed at the time of the creation of the Materials; **"JoVE"** means MyJoVE Corporation, a Massachusetts corporation and the publisher of The Journal of Visualized Experiments; **"Materials"** means the Article and / or the Video; **"Parties"** means the Author and JoVE; **"Video"** means any video(s) made by the Author, alone or in conjunction with any other parties, or by JoVE or its affiliates or agents, individually or in collaboration with the Author or any other parties, incorporating all or any portion

of the Article, and in which the Author may or may not appear.

2. **Background.** The Author, who is the author of the Article, in order to ensure the dissemination and protection of the Article, desires to have the JoVE publish the Article and create and transmit videos based on the Article. In furtherance of such goals, the Parties desire to memorialize in this Agreement the respective rights of each Party in and to the Article and the Video.

3. **Grant of Rights in Article.** In consideration of JoVE agreeing to publish the Article, the Author hereby grants to JoVE, subject to **Sections 4** and **7** below, the exclusive, royalty-free, perpetual (for the full term of copyright in the Article, including any extensions thereto) license (a) to publish, reproduce, distribute, display and store the Article in all forms, formats and media whether now known or hereafter developed (including without limitation in print, digital and electronic form) throughout the world, (b) to translate the Article into other languages, create adaptations, summaries or extracts of the Article or other Derivative Works (including, without limitation, the Video) or Collective Works based on all or any portion of the Article and exercise all of the rights set forth in (a) above in such translations, adaptations, summaries, extracts, Derivative Works or Collective Works and (c) to license others to do any or all of the above. The foregoing rights may be exercised in all media and formats, whether now known or hereafter devised, and include the right to make such modifications as are technically necessary to exercise the rights in other media and formats. If the "Open Access" box has been checked in **Item 1** above, JoVE and the Author hereby grant to the public all such rights in the Article as provided in, but subject to all limitations and requirements set forth in, the CRC License.

ARTICLE AND VIDEO LICENSE AGREEMENT

4. **Retention of Rights in Article.** Notwithstanding the exclusive license granted to JoVE in **Section 3** above, the Author shall, with respect to the Article, retain the non-exclusive right to use all or part of the Article for the non-commercial purpose of giving lectures, presentations or teaching classes, and to post a copy of the Article on the Institution's website or the Author's personal website, in each case provided that a link to the Article on the JoVE website is provided and notice of JoVE's copyright in the Article is included. All non-copyright intellectual property rights in and to the Article, such as patent rights, shall remain with the Author.

5. **Grant of Rights in Video – Standard Access.** This **Section 5** applies if the "Standard Access" box has been checked in **Item 1** above or if no box has been checked in **Item 1** above. In consideration of JoVE agreeing to produce, display or otherwise assist with the Video, the Author hereby acknowledges and agrees that, Subject to **Section 7** below, JoVE is and shall be the sole and exclusive owner of all rights of any nature, including, without limitation, all copyrights, in and to the Video. To the extent that, by law, the Author is deemed, now or at any time in the future, to have any rights of any nature in or to the Video, the Author hereby disclaims all such rights and transfers all such rights to JoVE.

6. **Grant of Rights in Video – Open Access.** This **Section 6** applies only if the "Open Access" box has been checked in **Item 1** above. In consideration of JoVE agreeing to produce, display or otherwise assist with the Video, the Author hereby grants to JoVE, subject to **Section 7** below, the exclusive, royalty-free, perpetual (for the full term of copyright in the Article, including any extensions thereto) license (a) to publish, reproduce, distribute, display and store the Video in all forms, formats and media whether now known or hereafter developed (including without limitation in print, digital and electronic form) throughout the world, (b) to translate the Video into other languages, create adaptations, summaries or extracts of the Video or other Derivative Works or Collective Works based on all or any portion of the Video and exercise all of the rights set forth in (a) above in such translations, adaptations, summaries, extracts, Derivative Works or Collective Works and (c) to license others to do any or all of the above. The foregoing rights may be exercised in all media and formats, whether now known or hereafter devised, and include the right to make such modifications as are technically necessary to exercise the rights in other media and formats. For any Video to which this **Section 6** is applicable, JoVE and the Author hereby grant to the public all such rights in the Video as provided in, but subject to all limitations and requirements set forth in, the CRC License.

7. **Government Employees.** If the Author is a United States government employee and the Article was prepared in the course of his or her duties as a United States government employee, as indicated in **Item 2** above, and any of the licenses or grants granted by the Author hereunder exceed the scope of the 17 U.S.C. 403, then the rights granted hereunder shall be limited to the maximum

rights permitted under such statute. In such case, all provisions contained herein that are not in conflict with such statute shall remain in full force and effect, and all provisions contained herein that do so conflict shall be deemed to be amended so as to provide to JoVE the maximum rights permissible within such statute.

8. **Protection of the Work.** The Author(s) authorize JoVE to take steps in the Author(s) name and on their behalf if JoVE believes some third party could be infringing or might infringe the copyright of either the Author's Article and/or Video.

9. **Likeness, Privacy, Personality.** The Author hereby grants JoVE the right to use the Author's name, voice, likeness, picture, photograph, image, biography and performance in any way, commercial or otherwise, in connection with the Materials and the sale, promotion and distribution thereof. The Author hereby waives any and all rights he or she may have, relating to his or her appearance in the Video or otherwise relating to the Materials, under all applicable privacy, likeness, personality or similar laws.

10. **Author Warranties.** The Author represents and warrants that the Article is original, that it has not been published, that the copyright interest is owned by the Author (or, if more than one author is listed at the beginning of this Agreement, by such authors collectively) and has not been assigned, licensed, or otherwise transferred to any other party. The Author represents and warrants that the author(s) listed at the top of this Agreement are the only authors of the Materials. If more than one author is listed at the top of this Agreement and if any such author has not entered into a separate Article and Video License Agreement with JoVE relating to the Materials, the Author represents and warrants that the Author has been authorized by each of the other such authors to execute this Agreement on his or her behalf and to bind him or her with respect to the terms of this Agreement as if each of them had been a party hereto as an Author. The Author warrants that the use, reproduction, distribution, public or private performance or display, and/or modification of all or any portion of the Materials does not and will not violate, infringe and/or misappropriate the patent, trademark, intellectual property or other rights of any third party. The Author represents and warrants that it has and will continue to comply with all government, institutional and other regulations, including, without limitation all institutional, laboratory, hospital, ethical, human and animal treatment, privacy, and all other rules, regulations, laws, procedures or guidelines, applicable to the Materials, and that all research involving human and animal subjects has been approved by the Author's relevant institutional review board.

11. **JoVE Discretion.** If the Author requests the assistance of JoVE in producing the Video in the Author's facility, the Author shall ensure that the presence of JoVE employees, agents or independent contractors is in accordance with the relevant regulations of the Author's institution. If more than one author is listed at the beginning of this Agreement, JoVE may, in its sole

ARTICLE AND VIDEO LICENSE AGREEMENT

discretion, elect not take any action with respect to the Article until such time as it has received complete, executed Article and Video License Agreements from each such author. JoVE reserves the right, in its absolute and sole discretion and without giving any reason therefore, to accept or decline any work submitted to JoVE. JoVE and its employees, agents and independent contractors shall have full, unfettered access to the facilities of the Author or of the Author's institution as necessary to make the Video, whether actually published or not. JoVE has sole discretion as to the method of making and publishing the Materials, including, without limitation, to all decisions regarding editing, lighting, filming, timing of publication, if any, length, quality, content and the like.

12. **Indemnification.** The Author agrees to indemnify JoVE and/or its successors and assigns from and against any and all claims, costs, and expenses, including attorney's fees, arising out of any breach of any warranty or other representations contained herein. The Author further agrees to indemnify and hold harmless JoVE from and against any and all claims, costs, and expenses, including attorney's fees, resulting from the breach by the Author of any representation or warranty contained herein or from allegations or instances of violation of intellectual property rights, damage to the Author's or the Author's institution's facilities, fraud, libel, defamation, research, equipment, experiments, property damage, personal injury, violations of institutional, laboratory, hospital, ethical, human and animal treatment, privacy or other rules, regulations, laws, procedures or guidelines, liabilities and other losses or damages related in any way to the submission of work to JoVE, making of videos by JoVE, or publication in JoVE or elsewhere by JoVE. The Author shall be responsible for, and shall hold JoVE harmless from, damages caused by lack of sterilization, lack of cleanliness or by contamination due to

the making of a video by JoVE its employees, agents or independent contractors. All sterilization, cleanliness or decontamination procedures shall be solely the responsibility of the Author and shall be undertaken at the Author's expense. All indemnifications provided herein shall include JoVE's attorney's fees and costs related to said losses or damages. Such indemnification and holding harmless shall include such losses or damages incurred by, or in connection with, acts or omissions of JoVE, its employees, agents or independent contractors.

13. **Fees.** To cover the cost incurred for publication, JoVE must receive payment before production and publication the Materials. Payment is due in 21 days of invoice. Should the Materials not be published due to an editorial or production decision, these funds will be returned to the Author. Withdrawal by the Author of any submitted Materials after final peer review approval will result in a US\$1,200 fee to cover pre-production expenses incurred by JoVE. If payment is not received by the completion of filming, production and publication of the Materials will be suspended until payment is received.

14. **Transfer, Governing Law.** This Agreement may be assigned by JoVE and shall inure to the benefits of any of JoVE's successors and assignees. This Agreement shall be governed and construed by the internal laws of the Commonwealth of Massachusetts without giving effect to any conflict of law provision thereunder. This Agreement may be executed in counterparts, each of which shall be deemed an original, but all of which together shall be deemed to be one and the same agreement. A signed copy of this Agreement delivered by facsimile, e-mail or other means of electronic transmission shall be deemed to have the same legal effect as delivery of an original signed copy of this Agreement.

A signed copy of this document must be sent with all new submissions. Only one Agreement is required per submission.

CORRESPONDING AUTHOR

Name:

Hanpeng Wang

Department:

Research Center of Geotechnical and Structural Engineering

Institution:

Shandong Univeristy

Title:

Professor

Signature:

Hanpeng Wang

Date:

2018.11.17

Please submit a **signed** and **dated** copy of this license by one of the following three methods:

1. Upload an electronic version on the JoVE submission site
2. Fax the document to +1.866.381.2236
3. Mail the document to JoVE / Attn: JoVE Editorial / 1 Alewife Center #200 / Cambridge, MA 02140

Dear Editor:

We wish to thank you for the time and effort you have spent reviewing our paper. We are pleased to note that you have found our research work interesting and also pointed out some problems to help us improve the quality of our work.

Motivated by your comments, we have deeply reconsidered the architecture of our work and tried to fix all the problems you mentioned. In particular, this revised manuscript of our resubmitted letter has significantly been improved mainly as follows: **(The reply is in red in this letter for your convenience)**

1. Please take this opportunity to thoroughly proofread the manuscript to ensure that there are no spelling or grammar issues.

Reply: Thanks for the comments. we have thoroughly checked and corrected the spelling and grammar mistakes in the revised manuscript.

2. Figure 1: The panel label D is hardly seen from the figure. Please use a different color for panel labels for better contrast.

3. Figure 2: Please mark the position where the sample is loaded. Please change the length unit “CM” to “cm”, and change “Led” to “LED”.

4. Figure 3 legend: It is unclear whether the height and diameter values are parameters of the material or the inner hole. Please clarify. Please also describe what the numbers represent.

5. Figures 6 and 7, Table 1: Please include a space between numbers and their corresponding units (0.0 MPa, 0.4 MPa, 2.0 MPa, 0-1 mm, 1-3 mm, etc.).

6. Table 2: Please apply superscript formatting to the number “3” in the unit “g/cm³”.

Reply: Thanks for the comments. We have rewritten the label in revised figures.

7. Table of Materials: Please sort the items in alphabetical order according to the name of material/equipment.

Reply: Thanks for the comments. We have revised the table of materials.

8. Please provide an email address for each author.

Reply: We have added the email address for each author in the revised manuscript.

9. Please include a space between all numerical values and their corresponding units: 15 mL, 37 °C, 48 h, 60 s; etc.

Reply: Thanks for the comments. We have corrected them in the revised manuscript.

10. Please add more details to your protocol steps. There should be enough detail in each step to supplement the actions seen in the video so that viewers can easily replicate the protocol. Please ensure you answer the “how” question, i.e., how is the step performed? Alternatively, add references to published material specifying how to perform the protocol action. See examples below.

Reply: Thanks for the comments. We have rewritten the protocol section and added more details in the revised manuscript.

11. 1.1: Please specify the size of the coal blocks that are collected.

Reply: Thanks for the comments. We have added the information in the revised manuscript. The details are as follows:

“Due to the low strength and looseness of structure, raw coal is broken and probably mixed with impurities. To avoid the influence of these internal and external factors as well as the inhomogeneity of coal as much as possible, select coal blocks (about 15 cm long, 10 cm wide and 10 cm high).”

12. 1.2: Please describe the cleaning procedure.

Reply: We have added details in the revised manuscript. The details are as follows:

“1.2. Use the tweezer to remove impurities mixed in coal and scrub the crusher chamber with absorbent cotton and acetaldehyde.”

13. 1.4: What is used to mix the powder?

Reply: We have added details in the revised manuscript. The details are as follows:

“1.4. Weigh 1000 g and 300 g of pulverized coal with particle size distribution of 0~1 mm and 1~ 3 mm respectively. Put them together into a beaker in a mass proportion of 0.76: 0.24 and mix them well with glass rod (diameter = 6 mm).”

14. 1.4 NOTE: $0.76/0.24 = 3.2$. Please explain how the size distribution value 0.25 is obtained.

Reply: We have added details in the revised manuscript. The details are as follows:

“1.4. Weigh 1000 g and 300 g of pulverized coal with particle size distribution of 0~1 mm and 1~ 3 mm respectively. Put them together into a beaker in a mass proportion of 0.76: 0.24 and mix them well with glass rod (diameter = 6 mm).

NOTE: According to the Gaudian-Schuman function of continuous packing theory, when particle size distribution value (m) equals approximate 0.25 (mass of particle size 1-3 mm: total mass = 0.24), the strength of briquette is maximal³⁰.”

15. 1.5: Is the mixture stirred?

Reply: We have added details in the revised manuscript. The details are as follows:

“1.5. To prepare the cement, put 4 g of sodium humate powder (99.99 % purity) into a beaker and add approximate 96 ml of distilled water. Use a glass rod to stir them and make sure that all sodium humate is well dissolved. The concentration of cement directly affects the compressive strength of briquette. **Table 1** reveals specific ratios of

briquette preparation, in which NO.2 sample has been used for representative results.”

16. 1.8: What is measured?

Reply: We have added details in the revised manuscript. The details are as follows:

“1.8. Put briquette in 40 °C incubator for 48 h. Then, weigh its mass with electronic scales (precision 0.01 g) and measure its height and diameter with vernier caliper (precision 0.02 mm) after drying.
”

17. 2.2.1: Please specify the monitoring time.

Reply: We have rewritten this part in the revised manuscript.

18. 2.2.2: Please reference Figure 2 for the position of valves.

Reply: We have rewritten this part in the revised manuscript.

“2.2.2. Start the vacuum pump. Open the valve V1 (**Figure 2**) and close V2, V3, V4 (**Figure 2**). Vacuumize the visualized vessel chamber. Turn off V 1 and vacuum pump until it is under vacuum.”

19. 2.3.1: Please describe how this is actually done.

Reply: We have added more details in the revised manuscript. The details are as follows:

“2.3.1. Measure the height (h) and diameter (d) of briquette with vernier caliper (precision=0.02 mm). Weigh the mass (m) of briquette with electronic scales (precision=0.01 g), and calculate its apparent density (ρ) by equation:

$$\rho = \frac{4m}{\pi d^2 h}.”$$

20. 2.3.4: Please describe how to create a new task.

Reply: We have added more details in the revised manuscript. The details are as follows:

“2.3.7. Start the software *SDU deformation acquisition V2.0* (or equivalent) to monitor circumferential deformation of briquette. Click on “Start”.”

Dear Reviewers:

We wish to thank you for the time and effort you have spent reviewing our paper. We are pleased to note that you have found our research work interesting and also pointed out some problems to help us improve the quality of our work.

Motivated by your comments, we have deeply reconsidered the architecture of our work and tried to fix all the problems you mentioned. In particular, this revised manuscript of our resubmitted letter has significantly been improved mainly as follows: (The reply is in red in this letter for your convenience)

Introduction

1. The sentence "The pore and fracture are partly connected and have a large specific surface area, which plays a vital role in gas sequestration and flow" requires more explanation and references. (Line No. 53-54)

Reply: Thanks for the comments. We have added the explanation and references in the revised manuscript. The details are as follows:

"The pore structure has a large specific surface area, which can adsorb a large amount of gas, playing a vital role in gas sequestration, and the fracture is main path for free gas flow^{7,8}."

In fact, coal is a natural adsorbent. The inner surface area of pore whose size is under 10^{-6} cm accounts for more than 98% of the total surface area, even up to $200 \text{ m}^2/\text{g}$ [R1, R2]. This structure leads to strong adsorption capacity of gas. The fractures in coal provide the path for free gas flow.

Reference 1: Nie, B. S., Li, X. C., Cui, Y. J. *Theory and application of gas migration in coal seam*. Science Press. Beijing (2014).

Reference 2: Scott, Ar. *Improving coal gas recovery with microbially enhanced coalbed methane. Coalbed Methane: Scientific, Environmental and Economic Evaluation*. Springer. Netherlands (1999).

2. The sentence "According to principles of orthogonal experimental method, the briquette, which is reconstituted with raw coal powder and cement, is regard as an ideal material used in the coal sorption test" requires references. (Line No. 66-68)

Introduction

Reply: Thanks for the comments. We have added the references in the revised manuscript.

3. Author has mentioned that "This glass has been successfully tested and proved to resist up to 10 MPa gas with low expansion rate, high strength, light transmittance and

chemical stability" but lack of any information about the testing report, standard followed etc. (Line No. 99-101)

Reply: Thanks for the comments. We have added the reference in the revised manuscript.

Sample Preparation

1. Include the mine data like Mine Location, Depth of coal seam etc. (Line No. 113)

Reply: Thanks for the comments. We have added the mine data in the revised manuscript. The details are as follows:

“The raw coal was taken from 4671B6 working face in Xinzhuangzi Coal Mine, Huainan, Anhui Province. The coal seam is approximately 450m below ground level and 360 m below sea level, and it dips at about 15 ° and is approximately 1.6 m in thickness.”

2. Specify the internal and external factors. (Line No. 114)

Reply: Thanks for the comments. We have added the information in the revised manuscript. The details are as follows:

“Due to the low strength and looseness of structure, raw coal is broken and probably mixed with impurities. To avoid the influence of these internal and external factors as well as the inhomogeneity of coal as much as possible, select coal blocks (about 15 cm long, 10 cm wide and 10 cm high).”

3. Why the samples were screened 6 to 16 mesh. Specify the standard with clear explanation. (Line No. 118)

Reply: Thanks for the comments.

In fact, the grain size distribution has an important effect on internal friction angle of material ^[R3-R5]. Based on the previous test results of similar material for methane-bearing coal, the angle of internal friction remains stable and is similar to that of raw in this size distribution (0~1 mm: 1~3 mm≈0.76:0.24) ^[R6]. In order to get these two sizes of coal powder, samples are screened 6 to 16 mesh.

Reference 3: Corriveau, D., Savage, S. B., Oger, L. *Internal Friction Angles: Characterization Using Biaxial Test Simulations*. Springer International Publishing, Netherlands (1997).

Reference 4: Shinohara, K., Oida, M., Golman, B. Effect of particle shape on angle of internal friction by triaxial compression test. *Powder Technology*. **107**(1), 131-136 (2000).

Reference 5: Dong, J. Y., Yang, J. H., Yang, G. X., Wu, F. Q., Liu, H. S. Research on similar material proportioning test of model test based on orthogonal design. *Journal of*

China Coal Society. **37**(1), 44-49 (2012).

Reference 6: Wang, H. P. et al. Development of a similar material for methane-bearing coal and its application to outburst experiment. *Rock and Soil Mechanics*. **36**(6), 1676-1682 (2015).

4. Mention the size of the briquette with standard and references. (Line No. 136)

Reply: Thanks for the comments. The briquette sample is cylindrical with a height of 100 mm and a diameter of 50 mm. which is the recommended size suggested by ISRM for uniaxial compression test^[R7]. We have added the reference in the revised manuscript.

Reference 7: Ulusay, R. *The ISRM Suggested Methods for Rock Characterization, Testing and Monitoring: 2007-2014*. Springer International Publishing. Switzerland (2015).

5. Justify the sentence "Set the loading mode to constant displacement at a rate of 0.5 mm/min. Press the briquette material under 15 MPa for 15 min, then unload" with standard and references. (Line No. 143-144)

Reply: Thanks for the comments. There a lot of research on briquette and its application on adsorption test ^[R8-R12]. Based on the scheme they adopted in briquette preparation, we made sample by cold pressing under 15 MPa in 15 min. The density becomes stable under this pressure or above^[R6]. In addition, the size of briquette made under this pressure is close to the standard size (height = 100 mm, diameter = 50 mm).

Reference 8: Xu, J., Ye, G. B., Li, B. B., Cao, J., Zhang, M. Experimental study of mechanical and permeability characteristics of moulded coals with different binder ratios. *Rock and Soil Mechanics*. **36**(1), 104-110 (2015).

Reference 9: Zhang, D. M., Hu, Q. T., Yuan, D. J. An experiment research on gas seepage of standard coal briquette specimen. *Jounral of China Coal Society*. **36**(2), 288-292 (2011).

Reference 10: Yin, G. Z., Wang, D. K., Zhang, D. M., Wang, W. Z. Test analysis of deformation characteristics and compressive strengths of two types of coal specimen containing gas. *Chinese Journal of Rock Mechanics and Engineering*. **28**(2), 410-417 (2009).

Reference 11: Skoczylas, N., Dutka, B., Sobczyk, J. Mechanical and gaseous properties of coal briquettes in terms of outburst risk. *Fuel*. **134**, 45-52 (2014).

Reference 12: Skoczylas, N. Laboratory study of the phenomenon of methane and coal outburst. *International Journal of Rock Mechanics and Mining Sciences*. **55**(10), 102-107 (2012).

6. Justify the sentence "Put briquette samples in 40°C incubator for 48h. Then, weigh and measure the samples after 148 drying." with standard and references. (Line No. 147-148)

Reply: Thanks for the comments. According to the curves of specimen drying time (figure 1), when the briquette was put in 40 °C incubator for drying, its mass becomes stable after 48 h. however, it would cost 7 days for sample drying in natural conditions (temperature 20 °C, relative humidity 65 %). To minimize the test time, the sample were put in incubator after cold press.

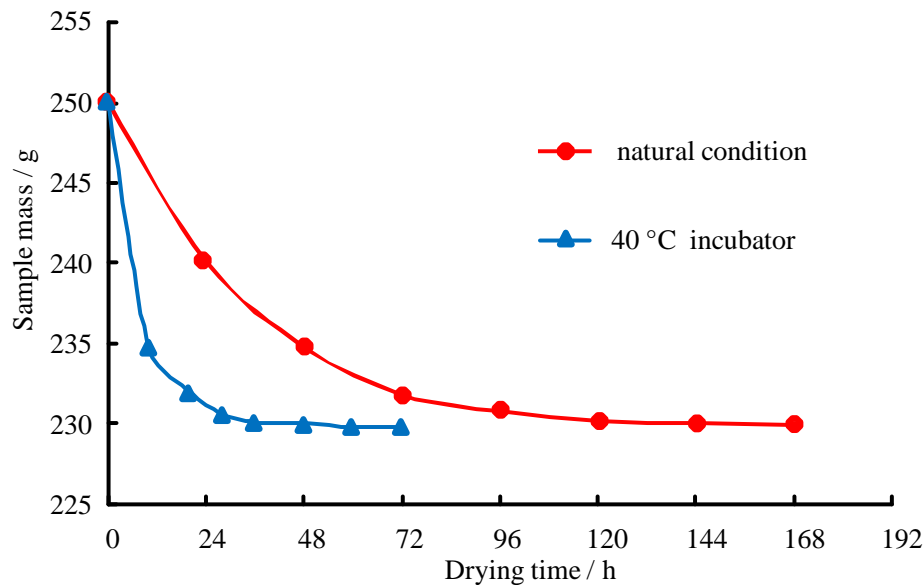


Figure 1 Curves of sample drying time

Experimental Methods

1. Justify the sentence "Set the moving ratio at 0.5mm/min and save the stress-strain curve." with standard and references. (Line No. 175-176)

Reply: Thanks for the comments. Based on the GB/T 15622-2005, the minimum pressure of loading piston was tested and it was translated into the stress value applied on the sectional area of sample in stress-strain curve according to the equation $\sigma = \frac{f}{S}$

(where the σ is the stress, f is the friction force and S is the sectional area of sample).

During data processing, all the axial stress-strain curves need to subtract the stress value mentioned above to demonstrate the real axial stress on the sample. In fact, the moving ratio should be the same as that of uniaxial compression test in order to control variables. We have corrected the loading ratio of uniaxial compression experiment in the revised manuscript.

2. Include the different physical experimental setup showing progress of work instead of only giving the animated 3-D model.

Reply: Thanks for your suggestions. We have added the physical pictures of experimental system in the revised manuscript.

3. Include appropriate labels in all the figures.

Reply: Thanks for the comments. We have reorganized the labels in figures in the revised manuscript.

Uniaxial Compression Experiment

1. Author has mentioned the loading in displacement mode with the rate of 1 mm/min. Please justify the rate of loading with references. (Line No. 200-201)

Reply: Thanks for the comments. There is a number of research about the effect of loading rate on rock mechanical behavior. Li H.T. et al. ^[R13] said the strength of coal increase firstly and decrease later with the increase of loading rate and the turning point of rate is named as critical loading rate; Qi C.Z. et al. ^[R14] concluded the peak strength of rock increases firstly and remain stable with the increase of loading rate. In this paper, in order to control rate variable and make sure it has less effect on the result comparison, the loading rate of uniaxial compression test was a constant during test. Meanwhile, considering of the relative low strength and large deformation of sample, the rate (1 mm / min) is moderate and meets the demand of test ^[R15- R18]. It takes approximately 6 minutes to complete test on average.

Reference 13: Li H. T., Jiang, C. X., Jiang, Y. D., Wang, H. W., Liu, H. B. Mechanical behavior and mechanism analysis of coal samples based on loading rate effect. *Journal of China University of Mining and Technology*. **44**(3), 430-436 (2015).

Reference 14: Qi, C., Wang, M., Bai, J., Wei, X. K., Wang, H. S. Investigation into size and strain rate effects on the strength of rock-like materials. *International Journal of Rock Mechanics and Mining Sciences*, **86**, 132-140 (2016).

Reference 15: Lajtai, E. Z., Duncan, E. J. S., Carter, B. J. The effect of strain rate on rock strength. *Rock Mechanics and Rock Engineering*. **24**(2), 99-109 (1991).

Reference 16: Wasantha, P. L. P., Ranjith, P. G., Zhao, J., Shao, S. S., Permathe, G. Strain Rate Effect on the Mechanical Behaviour of Sandstones with Different Grain Sizes. *Rock Mechanics and Rock Engineering*. **48**(5), 1883-1895 (2015).

Reference 17: Peng, F. L., Li, F. L., Li, J. Z., Kongkitkul, W., Tatsuoka, F. Visco plastic behaviors and constitutive modeling of sands under change of loading rates. *Chinese Journal of Rock Mechanics and Engineering*. **27**(8), 1576-1585 (2008).

Reference 18: Ma, S. P., Zhou, H. Surface strain field evolution of rock specimen under failure process. *Chinese Journal of Rock Mechanics and Engineering*, **27**(8), 1667-1673 (2008).

2. Rewrite the sentence "Store the images of briquette deformation during test". (Line No. 205-206)

Reply: Thanks for the comments. We have rewritten the sentence in the revised manuscript. The details are as follows:

“Save the sample images during loading”

3. What is Aviation Plug? Indicate in the figure with proper labeling. (Line No. 207)

Reply: The aviation plug is a kind of connector set in both loading vessel chamber and bottom plate for sensor connection for circumferential deformation apparatus. We have indicated it in the figure 2 in the revised manuscript.

REPRESENTATIVE RESULTS

1. Include the standard of briquette and mention its size. (Line No. 213)

Reply: Thanks for the comments. In fact, there is no widely accepted standard for briquette making. Many methods have been proposed by different scholars to prepare the briquette. When it comes to the rationale of sample in this paper, the briquette is proved as a similar material for raw coal in terms of mechanical properties and adsorption characteristics, and it has been successful applied in the coal and gas outburst physical simulation test^[R6, R19]. That is the reason why this scheme of briquette preparation was adopted.

The briquette sample is cylindrical with a height of 100 mm and a diameter of 50mm. which is the recommended size suggested by ISRM for uniaxial compression test^[R6]. The unevenness of sample end faces is less than 0.02mm.

Reference 19: Wang, H. P. et al. Coal and gas outburst simulation system based on CRISO model. *Chinese Journal of Rock Mechanics and Engineering*. **34**(11), 2301-2308 (2015).

2. Author has not mentioned anywhere about the standard method and procedure to measure Moisture Content, Ash Content and Volatile Matter. Include the standard procedure the section Experimental method. (Line No. 214-215)

Reply: We are very sorry for our negligence of these test methods. We have added the information in the revised manuscript. The details are as follows:

“1.9. Measure the moisture content, ash content and volatile content of briquette using a proximate analyzer (see Table of Materials) at a temperature of 20 °C and a relative humidity of 65 % (per standard GB/T 212-2008). Perform a vitrinite reflectance measurement on polish briquette using a photometer microscope (per standard GB/T 6948-2008).”

3. The statement "All the chemical components of briquette are similar to raw coal" is not clear. As the author mention earlier that the briquette is composed of coal and sodium humate solution then how the chemical components of briquette are similar to raw coal (Line No. 215)

Reply: Thanks for the comments. In fact, the sodium humate is extracted from raw coal, and it also has adsorption capacity^[R6]. Thus, the components of briquette are similar to those of raw coal.

4. There is no information regarding chemical characteristics in Table 2. (Line No. 216)

Reply: Thanks for the comments. We are very sorry for our incorrect statement. We have rewritten the sentence in the manuscript. The details are as follows:

“Table 2 The comparison of industrial analysis parameters between briquette and raw coal”

5. The sentences "The mechanical properties of briquettes used in test inevitably manifest some differences. However, the discreteness is much less than raw coal samples and it has little influence on the comparison and analysis of experimental results." is not clear. Rewrite the sentences properly. (Line No. 218-220)

Reply: Thanks for the comments. We have rewritten the part in the revised manuscript.

6. Include machine/system generated stress-strain curve.

Reply: Thanks for the comments. We have added the stress-strain curves (figure 2) in the revised manuscript.

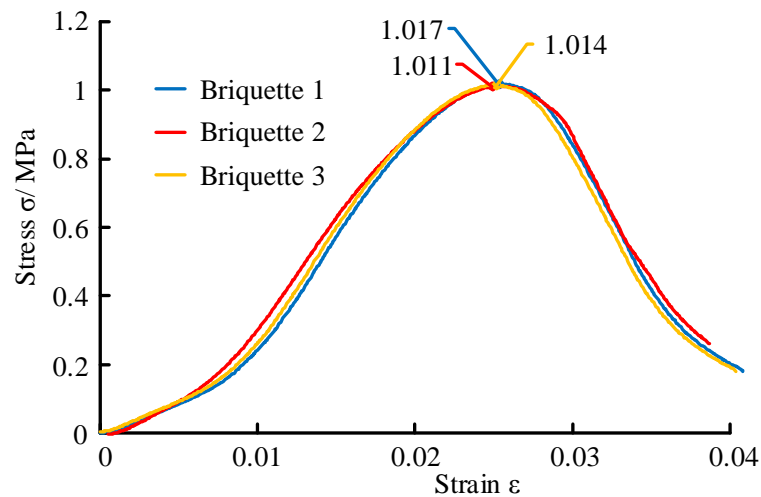


Figure 2 full stress-strain curves generated from test system using briquette

7. Include the mathematical equation used to determine different parameters.

Reply: Thanks for the comments. We have added the mathematical equations to calculate strength and elastic modulus reduction rate, fractal dimension and correlation coefficients in the revised manuscript.

8. How the strength reduction rate was calculated.

Reply: Thanks for the comments. From the stress-strain curves, the peak strength of sample was obtained. According to the equation $r = \left(1 - \frac{\sigma_{\max}}{\sigma_0}\right) \times 100\%$ (where the r is

strength reduction rate, σ_{\max} is the peak strength of sample under different pressure CO₂ and σ_0 is the peak strength of sample in atmospheric air), the reduction rate was calculated.

9. Justify the nonlinear correlation between strength reduction rate and gas pressure with proper references.

Reply: Thanks for the comments. Because of the space limits and requirement of journal, the relationship is not mainly discussed. The trend curve shows better agreement with data obtained from experiments using polynomial fitting than that using linear fitting. And this result has good conformity with previous experimental research [R20- R22].

In fact, the related theory research on constitutive model of gas-bearing coal shows that the relationship between coal strength and gas pressure is not linear [R23-R25]. For example: Base on the Gibbs free energy theory and Criterion of Griffith's Initial Fracturing, the equation between gas pressure, adsorption quantity and coal strength can be presented as follows^[R26]:

$$\left(\frac{\sigma_c}{\sigma_0}\right)^2 = 1 - \frac{RT}{\gamma_0 V_0 S} \int_0^p \frac{V}{p} dp \quad (1)$$

(where the σ_c is the tensile strength of coal; σ_0 is the tensile strength of coal in vacuum condition; R is the universal gas constant; T is the absolute temperature; γ_0 is the surface free energy of coal in vacuum condition; V_0 is the volume of molar vapor, 22.4L/mol in standard condition; S is the specific surface area; p is the gas pressure and V is the adsorption quantity). As the gas pressure increases, the coal strength will decrease according to the equation (1). Thus, it is a nonlinear correlation between them.

Reference 20: Masoudian, Mohsen, S., D. W. Airey, A. El., Zein. Experimental investigations on the effect of CO₂ on mechanics of coal. *International Journal of Coal Geology*. **128-129**, 12-23 (2014).

Reference 21: Zhao Y., Li X. H., Lu Y. Y., Kang Y. Influence of gas pressure on compressive strength size effect of inhomogeneous coal. *Journal of China Coal Society*.

34(8), 1081-1085 (2009).

Reference 22: Xu J. et al. An experimental study on the mechanical property of the gas-filled coal. *Journal of Chongqing University*. **16**(5), 42-47 (1993).

Reference 23: Zhu, W. C. et al. Impact of gas adsorption-induced coal damage on the evolution of coal permeability. *International Journal of Rock Mechanics and Mining Sciences*. **101**, 89-97 (2018).

Reference 24: Ranjith, P. G., Jasinge, D., Choi, S. K., Mehic, M., Shannon, B. The effect of CO₂ saturation on mechanical properties of Australian black coal using acoustic emission. *Fuel*. **89**(8), 2110-2117 (2010).

Reference 25: Viete, D. R., Ranjith, P. G. The effect of CO₂, on the geomechanical and permeability behaviour of brown coal: Implications for coal seam CO₂ sequestration. *International Journal of Coal Geology*. **66**(3), 204-216 (2006).

Reference 26: He, X. Q., Wang E. Y., Lin H. Y. Coal deformation and fracture mechanism under pore gas action. *Journal of China University of Mining and Technology*. **25**(1), 6-10 (1996).

10. Author should correlate the data obtained from the experimental testing with literature for its validity.

Reply: Thanks for the comments. In fact, the coal strength or elastic modulus reduction by CO₂ saturation observed from experimental result has good conformity with the previous research ^[R20-R22, R27-R28]. And the similar results are also found in the experimental and numerical simulation test for methane-bearing coal ^[R21, R29]. In addition, the fractal characteristics of fracture evolution of gas-bearing coal has been proved by some scholars ^[R30-R32]. We have added the related reference in the revise manuscript.

Reference 27: Ranjith, P. G., M. S. A. Perera. Effects of cleat performance on strength reduction of coal in CO₂ sequestration. *Energy*. **45**(1), 1069-1075 (2012).

Reference 28: Perera, M. S. A., P. G. Ranjith, M. Peter. Effects of saturation medium and pressure on strength parameters of Latrobe Valley brown coal: Carbon dioxide, water and nitrogen saturations. *Energy*. **36**(12), 6941-6947 (2011).

Reference 29: Liang, B., Zhang, M. T., Pan, Y. S., Wang, Y. J. Experimental research on effects of gas on mechanical properties and mechanical response of coal. *Chinese Journal of Geotechnical Engineering*. **17**(5), 12-18 (1995).

Reference 30: Cao, S. G. et al. Development of cracks in the process of coal destruction. *Journal of China University Mining and Technology*. **42**(5), 725-730 (2013).

Reference 31: Peng, S. J., Xu, J., Zhang, C. L., Feng, D., Nie, W. Fractal characteristics of crack evolution in gas-bearing coal under shear loading. *Journal of China Coal Society*. **40**(4), 801-808 (2015).

Reference 32: Chen, P. et al. Fractal characteristics of surface crack evolution in the process of gas-containing coal extrusion. *International Journal of Mining Science and Technology*. **23**(1), 121-126 (2013).

11. The term "initial damage" is not clear. (Line No. 340)

Reply: We are sorry for the incorrect statement. We have made correction in the revised manuscript. The details are as follows:

“Rock is a kind of solid medium and various external effects will cause damage in it.

12. Include the Conclusion section in the manuscript.

Reply: Thanks for the comments. It is really reasonable as reviewer suggested that a conclusion section should be included in the manuscript. However, JoVE is a method-based journal and there is no single section for conclusion according to the instruction of manuscript template. Instead, the representative results section proves the effectiveness of test method and the discussion section discusses the critical steps, modifications, limitations and application of the method. The conclusion of test method is included in the discussion section, and we have rewritten the part in the revised manuscript.

Dear Reviewers:

We wish to thank you for the time and effort you have spent reviewing our paper. We are pleased to note that you have found our research work interesting and also pointed out some problems to help us improve the quality of our work.

Motivated by your comments, we have deeply reconsidered the architecture of our work and tried to fix all the problems you mentioned. In particular, this revised manuscript of our resubmitted letter has significantly been improved mainly as follows: (The reply is in red in this letter for your convenience)

1. In protocol, more details, such as isothermal adsorption-desorption curves, compressive strength fluctuation curve and unevenness of sample end faces, are need to fulfill the information of briquette sample.

Reply: Thanks for the comments. We have added the isothermal adsorption curves, strength fluctuation curves in the revised manuscript, and the unevenness of sample end faces is about 0.02mm on average.

2. I wonder whether the pressure reduction rate (5%) in air tightness test are high to maintain the gas pressure stable.

Reply: Thanks for the comments. The air tightness was carried out based on the Chinese national standard GB150-2011, and the reduction rate meets the requirement of standard. In fact, the real pressure reduction rate is 1% under 2MPa CO₂.

3. Table 2, Author should provide information about type, locality of raw coal.

Reply: We are sorry for the negligence of information about raw. We have added the related data in the revised manuscript. The details are as follows:

“The raw coal was taken from 4671B6 working face in Xinzhuangzi Coal Mine, Huainan, Anhui Province. The coal seam is approximately 450m below ground level and 360 m below sea level, and it dips at about 15° and is approximately 1.6 m in thickness.”

4. It is recommended to present binary images of fractures only in white and black colors so that they succinctly reflect the covering area of fracture on sample.

Reply: Thanks for the suggestions. In fact, the different colors may demonstrate different fractures in different areas on coal sample. It is easy to distinguished for readers.

5. I wonder whether in the introduction the Authors could add some more references on the existing research about optical monitoring and coal's properties analysis.

Reply: hanks for the comments. We have added the references in discussion section the revised manuscript.

Dear Reviewers:

We wish to thank you for the time and effort you have spent reviewing our paper. We are pleased to note that you have found our research work interesting and also pointed out some problems to help us improve the quality of our work.

Motivated by your comments, we have deeply reconsidered the architecture of our work and tried to fix all the problems you mentioned. In particular, this revised manuscript of our resubmitted letter has significantly been improved mainly as follows: (The reply is in red in the revised letter for your convenience)

1. I think the most interesting thing is this work is the visualized and constant volume gas-solid coupling test system. However, in the line "84" of the manuscript, the authors added a review (review 24) there. I am failed to find this review, but from the name of this literature, I think it is closely related to this work. So, the difference between these two papers should be illustrated.

Reply: Thanks for the comments. In fact, the review 24 focus on the system introduction and related experiment analysis. Most importantly, its application tests are different from the test in this paper. In fact, JoVE is a method-based journal. This paper aims to present the whole procedure of test and provide this experimental method for readers, which lies in the requirement of method-based journal. Additionally, the test apparatus and method have been great improved and become more concise and accurate. Thus, there are no interest conflict between two papers.

2. In this work, the authors take a lot of space to illustrate how to prepare the standard briquette sample. But as far as I know, many methods have been proposed by different scholars to prepare the briquette, and no related standard has been widely accepted. Under different press pressure, press time, coal particle size, water content and additive, the physical and mechanical properties of the briquette sample would be rather different. This is the reason that the briquette sample is seldom used currently, although it a little dispersion degree as stated by the authors. So why you choose the particle size, the press pressure and press time in your work? And why this is the standard?

Response: Thanks for the comments. I agree with your opinion that the properties of briquette are different as there is no widely accepted sample preparation standard. An effective approach to investigate the mechanism of coal outburst is to conduct model test using similar materials. Based on this experiment objective, the briquette in this paper was initial developed for coal and gas outburst physical simulation test. The related test (figure 1, table 1) and isothermal adsorption test (figure 2) showed that the briquette performs well in mechanical properties and adsorption capacity with raw coal. Moreover, the briquette has been used to successfully reveal the phenomenon and process of methane outburst in model test ^[R1, R2]. Thus, this paper adopted the scheme of briquette preparation to carried out the related test.

As for the standard of briquette, we are very sorry for our incorrect statement. In fact,

it only means that the briquette sample is cylindrical with a height of 100 mm and a diameter of 50mm. which is the standard size suggested by ISRM for uniaxial compression test^[R3]. We have rewritten this relevant part in the revised manuscript.

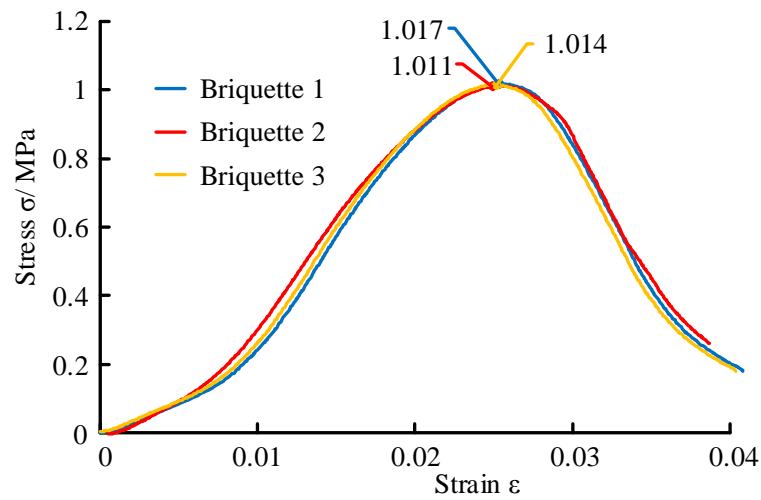


Figure 1 Full stress-strain curves generated from test system using briquette

Sample	Uniaxial compressive strength / MPa	Elastic modulus / GPa	Tensile strength / MPa	Internal friction angle / °	Cohesion / MPa	Pission ratio
raw coal	25.23	4.529	2.30	30	0.800	0.25
briquette	1.011	0.067	0.11	29	0.117	0.25

Table 1 The mechanical characteristics of raw coal and briquette

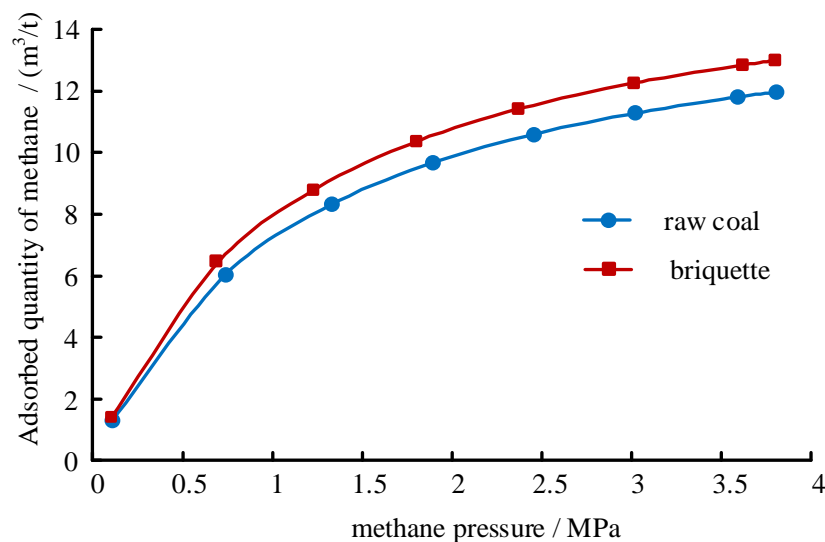


Figure 2 Comparison of adsorption capacity between raw coal and briquette

Reference 1: Wang, H. P. et al. Development of a similar material for methane-bearing coal and its application to outburst experiment. *Rock and Soil Mechanics*. **36**(6), 1676-

1682 (2015).

Reference 2: Wang, H. P. et al. Coal and gas outburst simulation system based on CRISO model. *Chinese Journal of Rock Mechanics and Engineering*. **34**(11), 2301-2308 (2015).

Reference 3: Ulusay, R. *The ISRM Suggested Methods for Rock Characterization, Testing and Monitoring: 2007-2014*. Springer International Publishing. Switzerland (2015).

3. In the discussion part, the related analysis and discussion are rather poor. Generally speaking, this part is the most important part of the paper. Therefore, the discussion part is required to be further analyzed.

Reply: Thanks for the comments. It is really reasonable as reviewer suggested that the discussion is the most important section in the paper. As JoVE is a method-based journal. Therefore, the discussion section is required to focus on protocol including the critical steps, modifications, limitations and future application of the method rather than the representative results. Based on such purpose, we have rewritten the part in the revised manuscript.

4. The English in this paper is very good on a whole, but many grammar errors can still be found.

Reply: Thanks for the comments. We have thoroughly checked and correct the spelling and grammar errors in the revised manuscript.

Dear Reviewers:

We wish to thank you for the time and effort you have spent reviewing our paper. We are pleased to note that you have found our research work interesting and also pointed out some problems to help us improve the quality of our work.

Motivated by your comments, we have deeply reconsidered the architecture of our work and tried to fix all the problems you mentioned. In particular, this revised manuscript of our resubmitted letter has significantly been improved mainly as follows: (The reply is in red in this letter for your convenience)

1. The experimental parts shown in the fig.2 should be explained in a clear order;

Reply: Thanks for the comments. We have reorganized the labels in a clear order in the revised manuscript.

2. Small parts displayed in the fig.4 should be marked in their places in the fig.2;

Reply: Thanks for the comments. We have marked the connecting tools in figure 2 in the revised manuscript

3. As we all know, the index of refraction of gas changes with the gas density. Thus, the images captured by the digital camera under different gas pressures are influenced by the dynamic index of refraction. However, in this paper, this was disregarded by authors;

Reply: Thanks for the comments. There are several factors, such as pressure, temperature and molar mass, affecting the index of gas refraction. In this test, the only variable is gas pressure. According to the previous tests on gas refraction, the index of refraction CO₂ changed little in 29.2 °C or even lower under 3MPa compared to that of CO₂ in standard state (0°C, 101.325kPa) ^[R1, R2]. As the maximum pressure is 2MPa in the test, the index of refraction can be seen as a constant (approximate 1.00045) during test. In addition, before the sample was loaded, the briquette has reached adsorption and desorption dynamic equilibrium., which means the density of CO₂ have been stable. And the optical monitoring only works during sample loading. The density of CO₂ in loading chamber will not change because of the constant volume structure. Thus, the index of refraction has little effect on the images capture.

However, when the pressure is relatively high and obviously changes the density of gas, the dynamic refraction needs to take into consideration during images capturing. We have added the related information in the revised manuscript.

Reference 1: Xia, G. Z. *Study on density and refractive index of near-critical fluid*. Master's degree Thesis. Huazhong University of Science and Technology. (2009).

Reference 2: Hyeon, S. B., J, T. In. Pressure-dependent refractive indices of gases by THz time-domain spectroscopy. *Optics Express*. **24**(25), 29040-29047 (2016).

4. In the line 226-227, the calculating process of elastic module was not clear. Please

add the stress-strain curves of the tests.

Reply: Thanks for the comments. We are very sorry for our incorrect statement. We have added the specific equation in the revised manuscript. The details are as follows:

“The linear stage in axial stress-strain curves was used to calculate the elastic modulus according to equation $E = \frac{\Delta\sigma}{\Delta\varepsilon}$ (where E is the elastic modulus; $\Delta\sigma$ is the stress increment of linear stage, MPa; $\Delta\varepsilon$ is the strain increment of linear stage)”

The stress-strain curves of test were presented in figure 8 (A), where stress-axial strain, stress-circumferential strain and stress-volume strain curves are included.

5. Too many words about the cautions of experiments in the discussion. I strongly recommend to add a section to state the cautions;

Reply: Thanks for the suggestions. We have combined these cautions in protocol in the revised manuscript.

6. The discussion is not incisive. More words are needed to explain the phenomenon in the results;

Reply: Thanks for the comments. It is very reasonable that an article should put more emphasis on the analysis of test phenomenon in the discussion. As JoVE is a methods-based journal. This article aims to demonstrate the experimental method using the test system. According to the instruction and requirement of journal proposal, the discussion section of article focuses on the protocol including critical steps, modifications, limitations and future application of the method rather than the representative results. Based on such purpose, we have rewritten the part in the revised manuscript.

7. No conclusion in this paper, and the paper is not intact;

10. This paper is badly organized, for example, the apparatus instruction is placed in Instruction Section, the conclusion is missing;

Reply: Thanks for the comments. In the introduction of this paper, we included the purpose, advantages and context of the experimental method in introduction. In fact, the apparatus is an important part of the method. The information about apparatus could help readers achieve better understanding. That is reason why we placed the apparatus instruction in introduction.

Additionally, according to the instruction of manuscript of JoVE, there is no single conclusion section. Instead, the representative results section proves the effectiveness of test method and the discussion section discusses the critical steps, modifications, limitations and application of the method. The conclusion of test method is included in the discussion section, and we have rewritten the part in the revised manuscript.

8. Too many keywords were listed in this paper, five or six keywords may be suitable. Please simplify it;

Response: Thanks for the comments. We have simplified the key words in the revised manuscript.

9. Line 52, you stated that "Coal is a massive, structurally isotropic rock composed of pore, fracture and coal matrix", I do not agree with this view. In fact, the structure of pore, fracture and coal matrix makes coal anisotropic and heterogeneous;

Reply: Thanks for the comments. We are very sorry for our incorrect statement. The coal is anisotropic and heterogeneous. We have rewritten the sentence in the revised manuscript.

11. In "Section 1. Sample Preparation", you adopted coal briquette to replace the raw coal, indeed, the large raw coal is difficult to obtain from coal mines. But why you choose this formula (coal powder accounts for 92%, and cement accounts for 8%) to make the coal briquette, are the mechanical property or the adsorption capacity of coal briquette comparable to that of raw coal. You must conduct some tests to validate this question;

Reply: Thanks for the comments. according to the previous experimental phenomenon, when the cement account for less than 8%, the material is difficult to well mix, which lead to the low strength of briquette. When the cement accounts for more than 13%, the material is too wet to cold press. Moreover, considering of the dry time (figure 1), the formula (coal powder: cement = 92 %: 8 %) was chosen for briquette preparation.

As for the mechanical property and adsorption capacity, we have added the related test results including full stress-strain curves, tensile strength, Poisson ratio, cohesion force, internal friction angle tests and isothermal adsorption curves to prove the similarity between raw coal and briquette in the revised manuscript. Additionally, the briquette has been successfully used in model test for coal and gas outburst ^[R3, R4], which enhanced the validation.

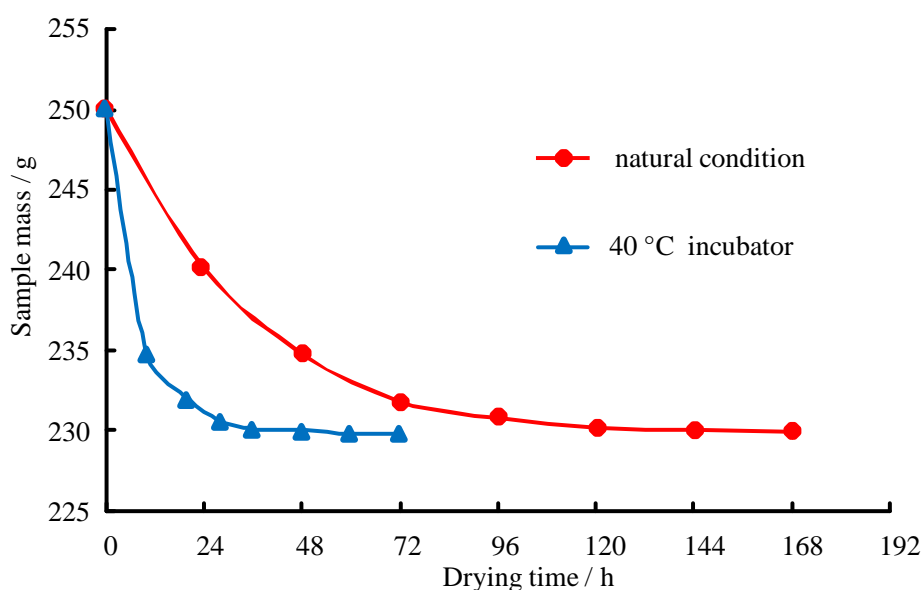


Figure 1 Curves of sample drying time

Reference 3: Wang, H. P. et al. Development of a similar material for methane-bearing coal and its application to outburst experiment. *Rock and Soil Mechanics*. 36(6), 1676-1682 (2015).

Reference 4: Wang, H. P. et al. Coal and gas outburst simulation system based on CRISO model. *Chinese Journal of Rock Mechanics and Engineering*. 34(11), 2301-2308 (2015).

12. There exists some syntax errors in the paper

Reply: Thanks for the comments. we have thoroughly checked and corrected the spelling and grammar mistakes in manuscript.